Positive effect of Mdm2 on p53 expression explains excitability of p53 in response to DNA damage

Ján Eliaš[a,b]

[a]*Laboratoire de Mathématiques d'Orsay, Univ. Paris-Sud, CNRS, Université Paris-Saclay, 91405 Orsay, France*
[b]*Sorbonne Universités, Inria, UPMC Univ Paris 06, Lab. J.L. Lions UMR CNRS 7598, Paris, France*

Abstract

Most of the existing biological models consider Mdm2 as a dominant negative regulator of p53 appearing in several negative feedback loops. However, in addition to targeting p53 for degradation, Mdm2 in tight cooperation with MdmX can control expression levels of p53 through enhanced induction of p53 synthesis in response to DNA damage. Whilst ATM-dependent phosphorylation of p53 is not observed to be important in this enhanced synthesis, ATM-dependent phosphorylation of Mdm2 (as well as MdmX) is essential for its dual role, which is accompanied with widely oscillating p53. In the light of these new observations we formulate a novel molecular mechanism which, *in silico*, is capable of triggering p53 oscillations. The mechanism that is based on Mdm2's dual regulation of p53 can provide mechanistic insights into an excitability of the p53 network, thus it contributes to understanding of variability of p53 dynamics in response to single and double strand breaks.

Keywords: p53, Mdm2, oscillations, excitability, reaction-diffusion model

1. Introduction

The tumour suppressor protein p53 is activated in response to a variety of stimuli and it acts primarily as a transcription factor for many downstream genes. Protein products of these genes, if possible, suppress fluctuations caused by the stimulus, and if not possible, initiate irreversible processes such as apoptosis or senescence in order to prevent a development of cancer. For further details, we refer to the reviews [64, 65, 66, 36, 38].

Email address: jan.elias@inria.fr (Ján Eliaš)

One of the downstream transcriptional targets of p53 is the E3 ubiquitin-protein ligase Mouse double minute 2 homolog (Mdm2; also known as Hdm2) which, in turn, regulates negatively the level and activity of p53 [29]. For instance, Mdm2 can interact with the amino-terminus of p53 in a region that disables p53 to bind DNA [49, 50, 69]. Mdm2 can further regulate p53 either through the mono-ubiquitination of p53, which is followed by the nuclear export of such labeled p53 molecules to the cytoplasm, or through the poly-ubiquitination and subsequent degradation of p53 [25, 39]; either way, ubiquitin-dependent processes mediated by Mdm2 remove p53 from its site of action. In fact, most of existing feedback loops that negatively regulate p53 include Mdm2 which is thus considered as a dominant negative regulator of p53 [24] and which is often amplified in cancer cells retaining the *p53* gene in its wild type (wt) configuration [47].

Although Mdm2 does not reduce the level of p53 mRNA, which remains fairly unchanged during protein signalling in several cancer cell lines with or without DNA damage [25, 33], Mdm2 can regulate p53 synthesis from its mRNA. In recent works [21, 44], R. Fåhraeus and his colleagues discovered and described a precise molecular mechanism of the positive role of Mdm2 and Mouse double minute 4 homolog (MdmX; also known as Mdm4 and HDMX) in the regulation of p53 after genotoxic stress. In particular, they observed that Mdm2 and MdmX are phosphorylated by the kinase Ataxia-Telangiectasia Mutated (ATM), a sensor of DNA double strand breaks (DSB), at the serine residues Ser395 [45] and Ser403 [44], respectively, hereafter denoted by Mdm2-P and MdmX-P. Both Mdm2-P and MdmX-P can bind and form complexes with the nascent p53 mRNA following genotoxic stress. Phosphorylated MdmX binds specifically to a newborn p53 mRNA in the first instance and promotes conformational changes in the mRNA in a way that favours attraction of Mdm2-P to the complex [44]. In such complexes, MdmX-P acts as the RNA chaperone during its transportation from the nucleus to the cytoplasm [44]. Phosphorylated Mdm2 in the complex stimulates p53 mRNA translation, Figure 1. In fact, Mdm2-P may induce more than a three-fold increase in the rate of p53 synthesis in H1299 cells, human non-small cell lung carcinoma cells, exposed to doxorubicin [21, 44]. Whilst Mdm2-P is less capable of ubiquitination of p53 expressed from a Mdm2 binding mRNA, wt p53 expressed from a non-Mdm2 binding mRNA is hyperunstable in the presence of Mdm2 in the DNA damage response (DDR) [21, 44].

ATM-dependent phosphorylation of Mdm2 and MdmX is required for p53

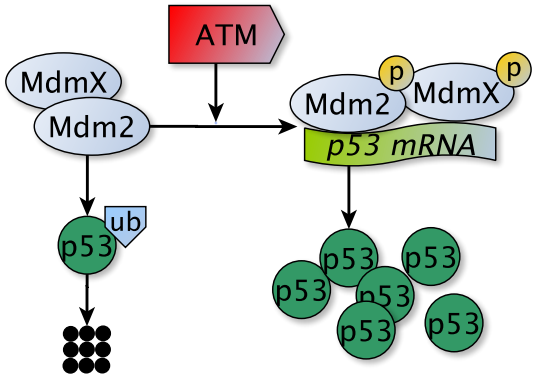

Figure 1: Depending on their phosphorylation status, if not phosphorylated by ATM, Mdm2 targets p53 for degradation, if phosphorylated by ATM, Mdm2-P and MdmX-P bind p53 mRNA and enhances its synthesis with a 3-4 fold increase in the synthesis rate [21]. *In this and following sketches, 'p' stands for a phosphate group attached to Mdm2 by ATM, 'ub' for a ubiquitin group attached to p53 by Mdm2; black dots represent peptides left after protein degradation.*

mRNA–MdmX–Mdm2 interactions. Indeed, while phosphorylation of Mdm2 by ATM promoted its interaction with p53 mRNA, non-phosphorylated Mdm2 had weak affinity for p53 mRNA [21]. Phosphorylation of either of the two proteins supports formation of Mdm2–MdmX oligomers; non-phosphorylated Mdm2 interacts with MdmX and prevents its RNA chaperone activity [44]. Mdm2's Ser395 phosphorylation site is sufficient and necessary for the stability of p53 mRNA–Mdm2 complexes with a 3-5 fold increased abundance of p53 mRNA bound to Mdm2-P following treatment of H1299 and AT5-BIVA (a fibroblast cell line with exogenous ATM) cells with doxorubicin [21]. In addition, ATM-dependent phosphorylation of Mdm2 was not followed by Mdm2-P rapid degradation in [21, 44] as it was observed in [59, 5]. Instead, this phosphorylation event led to an accumulation of Mdm2-P in the nucleoli where Mdm2-P likely changed its function from being a negative to a positive regulator of p53 [21].

On the other hand, almost all existing (biological and mathematical) models of the p53 dynamics assume that it is phosphorylation of p53 by ATM at Ser15 which enables p53 to escape from the Mdm2-dependent degradation,

to accumulate and stabilise in the nucleus [64]. Nevertheless, phosphorylation of p53 by ATM was not observed to be important for its stabilisation nor for the positive effect of Mdm2-P towards p53 expression in response to DNA damage [21]. In the line with these observations, close examination of all possible phosphorylation sites of p53 revealed that phosphorylation of Ser15 may not have any direct effects on Mdm2's binding to p53. Phosphorylation of the threonine residue Thr18 was the only event reducing significantly the ability of Mdm2 to bind p53 [57].

Taking these new evidences into consideration, we propose a novel molecular mechanism for the activation and regulation of p53 in the DDR. We show that this new mechanism reproduces *in silico* p53 oscillations observed after genotoxic stress. Indeed, in response to different (low, moderate and high) doses of DNA damaging agents causing DNA DSB, p53 oscillates in its concentration (with the fixed amplitude and period) in several cell lines, including cancerous cell lines such as MCF7, A549, U2-OS and HCT116 and non-transformed RPE1 cells [5, 12, 13, 22, 34, 40, 41]. In addition, p53 oscillations have been observed *in vivo* [23]. The mathematical model is based on the simple conclusions from above, see also Figure 2: as long as the ATM signalling is active, Mdm2-P and MdmX-P act as positive regulators of p53, whilst p53 is degraded by Mdm2 whenever Mdm2-P is dephosphorylated by Wild-type p53-induced phosphatase 1 (Wip1), another transcriptional target protein in the p53's downstream pathway [19, 42].

We show also that the model can provide mechanistic insights into some specific features of p53 dynamics, namely, excitability of p53. The network of p53 is an excitable system in response to DSB caused by γ-radiation or drugs, e.g., neocarzinostatin (NCS), [6, 5]. It is excitable even in non-stressed conditions in proliferating cells which may show spontaneous pulses of p53 associated with intrinsic DNA damage [40]. This means that a transient stimulus, for example, a short pulse of ATM is sufficient to trigger a full pulse of p53, Figure S2(a). Indeed, cells treated with ATM's inhibitor wortmannin (wm) one hour after DNA damage exhibit one full pulse of p53 [5]. On the other hand, response of the p53 network to UV-radiation is not excitable and it depends continuously on the signalling of the upstream kinase ATR, which is the activator of p53 pathway and the sensor of single strand breaks (SSB) caused by UV-radiation. ATR inhibited one hour post-irradiation results in the inhibition of p53 levels which remain fairly constant in the following time course [5], Figure S2(b).

The rest of the paper is organised as follows: in Section 2 a molecular

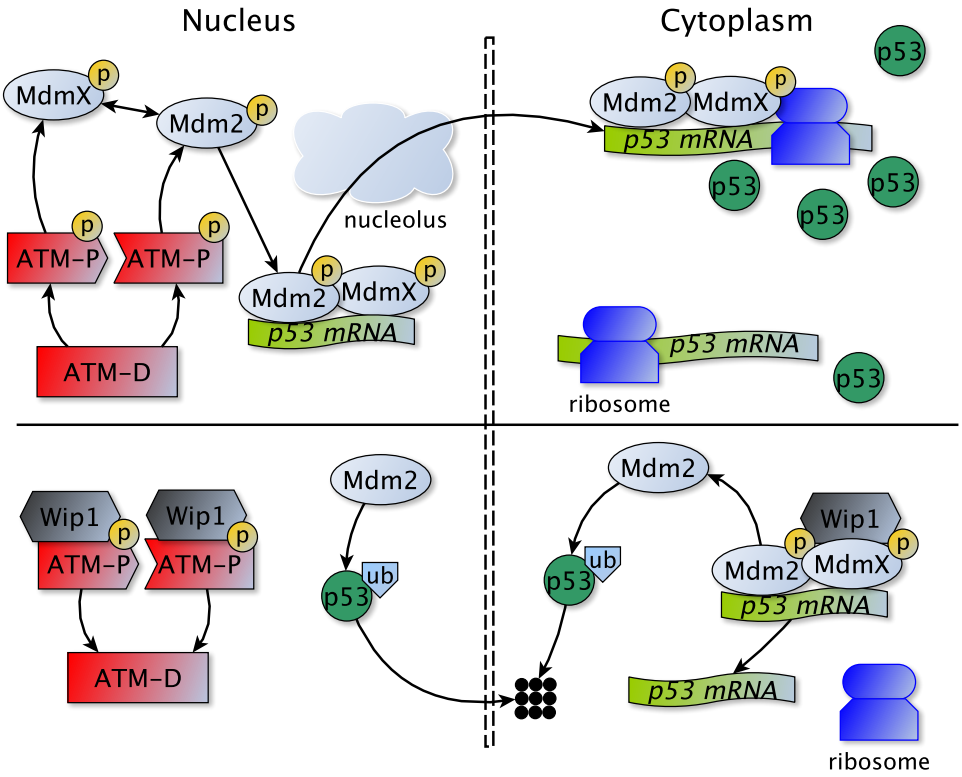

Figure 2: In the presence of DNA damage, inactive ATM dimers dissociate into active monomers [3], which phosphorylate Mdm2 at Ser395 and MdmX at Ser403 in the nuclear compartment [3, 72]. Mdm2-P and MdmX-P then form a complex with a nascent p53 mRNA at the DNA sites and move together from the nucleus to the cytoplasm, passing likely through the nucleolus where Mdm2 switches into a positive regulator of p53, i.e., Mdm2-P enhances p53 translation from its mRNA and, at the same time, Mdm2-P is less capable of p53 ubiquitination. This all enables p53 to accumulate in the nucleus where it acts as a transcription factor for the *Mdm2* and *Wip1* genes [4, 19]. The phosphatase Wip1 targets ATM-P for dephosphorylation and thus inactivation [58]. Wip1 reverses also Mdm2 and MdmX phosphorylation status, [70, 74], so that Mdm2 promotes ubiquitination and degradation of p53. The persistent DNA damage signal can trigger another pulse of p53 by ATM dimer monomerisation again.

model and assumptions for a mathematical reaction-diffusion (RD) system of Mdm2's dual regulation of p53 are introduced. The equations of the system are described in Supplemental Information (SI). In Section 3 we demonstrate that the model is capable of reproducing basic biological single cell observations, which are recalled consecutively. Section 3.4 is dedicated to the phenomenon of excitability of p53 and we propose a molecular mechanism in Discussion that could possibly explain it, formulated rather as a hypothesis to be verified by further experiments.

2. A novel mechanism for p53 oscillations

A molecular model for p53 oscillations is based on the recent observations published in [21, 44] as discussed in Introduction, i.e., a model is composed of the feedback loops $p53 \to Mdm2 \dashv p53$ and $ATM\text{-}P \to Mdm2 \to p53 \to Wip1 \dashv ATM\text{-}P$, see also Figures 2 and S5(b). In the schematic notation $A \to B \dashv C$, A positively regulates B whilst B negatively regulates C where by regulation we mean a regulation either of activity, expression or degradation of the object of regulation. For simplicity, we omit MdmX from the loops since MdmX acts hand in hand with Mdm2 and we do not consider specific conformational changes in the structure of p53 mRNA caused by MdmX by any means or any other activity of MdmX in the p53 network. Instead we assume that mRNA has a conformation which enables Mdm2-P association with the mRNA. However, this simplification does not change dramatically the overall dynamical scheme under consideration, compare Figures 2 and S1. Indeed, one can look at Mdm2-P in the sketch in Figure S1 as the complex of Mdm2-P and MdmX-P.

Following DNA damage and the presence of DNA DSB, inactive ATM dimers dissociate through auto-phosphorylation into active monomers (hereafter denoted by ATM-P) [3]. ATM-P molecules phosphorylate Mdm2 [45] and Mdm2-P then targets p53 mRNA instead of the protein p53 [21, 44]. The p53 mRNA–Mdm2 complex moves from the sites of mRNA transcription to the cytoplasm where Mdm2-P facilitates binding of the free ribosomes to the mRNA. The mRNA bound to the complex is then translated with an increased synthesis rate than the mRNA escaping Mdm2-P; both mRNAs giving the p53 protein [21, 44]. Phosphorylated Mdm2-P is also less efficient in the ubiquitination of p53 [45]. All this allows p53 to accumulate in the nucleus where it can act as a transcription factor for the $Mdm2$ [4], $Wip1$ [19] and many other genes. In turn, Wip1 dephosphorylates Mdm2-P and

dephosphorylated Mdm2 targets p53 for degradation. Wip1 also dephosphorylates ATM-P establishing thus homeostasis in the DDR [42]. This closes the first cycle between the antagonists. Since we do not consider any DNA repair mechanism nor activation of irreversible cell fates such as apoptosis or senescence, the persistent DNA damage signal triggers another wave of ATM-P and consequently pulses in all the other proteins.

2.1. Modelling Mdm2's dual function: mathematical formalism

From a mathematical point of view, we have extended the deterministic reaction-diffusion model developed in [17]. It is shown in [17] that the spatial representation of cellular environment combined with the negative feedback loops involving Mdm2 and Wip1 (see Fig. S5(a)) creates a realistic framework for the oscillatory dynamics of p53.

Protein-protein interactions (e.g., posttranslational modifications such as phosphorylation or ubiquitination) are modelled as the enzyme reaction

$$S + E \underset{k_-}{\overset{k_+}{\rightleftharpoons}} C \xrightarrow{k_{cat}} E + P$$

where the enzyme E converts the substrate S to the product P through a two-step process with the intermediate complex C. Following the mass action kinetics and quasi-steady-state approximation [30], we can derive an algebraic expression (Michaelis function) for the concentration (denoted by square brackets $[\cdot]$) of the substrate and the product

$$\frac{\mathrm{d}[S]}{\mathrm{d}t} = -\frac{\mathrm{d}[P]}{\mathrm{d}t} = -k_{cat} E_0 \frac{[S]}{K_M + [S]} \quad \text{with} \quad K_M = \frac{k_- + k_{cat}}{k_+} \tag{1}$$

which depends on two parameters: turnover k_{cat} and Michaelis K_M rate. Some parameters for reactions satisfying equation (1) with $V_M[\cdot]/(K_M + [\cdot])$ can be found in the literature. We take these experimental values (K_M and $k_{cat} \approx V_M$ with E_0 replaced by the actual concentration of $[E]$) for the reference rates for our reactions, though they may be inaccurate in the cellular context. Note that we aim at modelling spatio-temporal protein dynamics and not at the kinetics of chemical reactions themselves. Thus and similarly as some other authors in systems biology of signal transduction, e.g. [14, 43, 61, 73], we overgeneralise the use of Michaelis functions in our model and neglect the complexity of Michaelian enzymology from our consideration.

A simple gene regulatory circuit for some mRNA and its protein product P is represented by two equations

$$\frac{\mathrm{d}[mRNA]}{\mathrm{d}t} = I - \delta_{mRNA}[mRNA],$$
$$\frac{\mathrm{d}[P]}{\mathrm{d}t} = k[mRNA] - \delta_P[P],$$

where δ_{mRNA} and δ_P are degradation rates for mRNA and P, respectively, k is a rate of mRNA translation and I is a production (source) term for mRNA. It can be a constant or any other function, e.g., Hill function with the coefficient 4 used for the transcription of the $Mdm2$ and $Wip1$ genes [15, 16, 61].

2.2. Modelling Mdm2's dual function: assumptions

According to the generally accepted theory, the abundance of p53 is determined mainly by its degradation rate, rather than the rate at which it is produced [64]. Thus, almost all mathematical models, which adapt to this theory, do not consider explicitly any mRNA of p53. However, under the new circumstances relying on the synthesis of mRNA either bound or unbound to the phosphorylated Mdm2 protein, the concentration of p53 mRNA will be represented by a physiological variable, a real function rather than a constant.

In our previous spatial model [17], the cell was designed to consist of the two compartments: nucleus and cytoplasm. These compartments were separated by the endoplasmic reticulum (ER) where no translation of the mRNA was allowed, see [16, 17, 61] and citations therein. Since, phosphorylated Mdm2-P binds a nascent p53 mRNA at the transcription site in the nucleus, we specify a small area inside the nucleus, a "DNA locus", denoted by χ_L in Figure 3, similarly as it was specified in [60]. Every single (p53, Wip1 and Mdm2) mRNA is assumed to be made in χ_L. Further we assume that the reaction

$$p53\ mRNA + Mdm2\text{-}P \xrightarrow{k_a} C,$$

where C denotes the p53 mRNA–Mdm2-P complex and k_a is the association rate of this reaction, occurs in the DNA locus χ_L only. The complex C moves to the cytoplasm where it binds to free ribosomes localised outside of the ER. The complex C can dissociate back into p53 mRNA and Mdm2-P in the cytoplasm, thus following the reaction

$$C \xrightarrow{k_d} p53\ mRNA + Mdm2\text{-}P$$

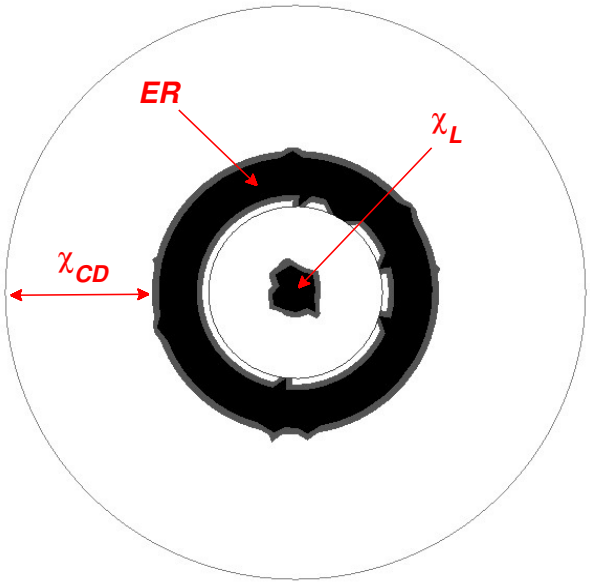

Figure 3: A scheme of the cell used in the model: the cell is represented by a disc with radius $10\,\mu m$. It consists of the nucleus represented by an inner disc of radius $3\,\mu m$ and the cytoplasm containing the rest of the cell. Within the cytoplasm there is the endoplasmic reticulum (ER) where no translation of the mRNAs occurs. The ER is represented by an annulus with radii $3\,\mu m$ and $5\,\mu m$. Translation of the mRNAs is supposed to occur outside of the ER, thus in an annulus χ_{CD} with radii 5 and $10\,\mu m$. Inside the nucleus there is a small "gene" subdomain χ_L of radius $1\,\mu m$ which represents the DNA locus where all production of mRNA content occurs.

with the dissociation rate k_d. Once it is released from C, we assume that p53 mRNA can be used again in the translation process, however, Mdm2-P cannot bind such mRNA again nor any other p53 mRNA outside of the DNA locus χ_L in the nucleus. The half-life $t_{1/2}$ of the complex C is set to 1 hour which is the same as the half-life of Mdm2 mRNA reported in [46] and 3-fold longer than the half-life of "free" p53 mRNA not bound to C, since, by following [2], the half-lives of mRNA of short-lived proteins such as transcription factors are often shorter than 30 minutes.

Further, we consider two copies of p53 made either from the free mRNA unbound to C (denoted by p53-1) or from the mRNA bound to C (denoted

by p53-2). From these, p53-2 is more stable than hyperunstable p53-1. To mimic this, less stable p53-1 is targeted for ubiquitination by Mdm2 with the turnover rate $k_{ub\text{-}1} = 5\, min^{-1}$ (the value taken from [35]) and by Mdm2-P with the rate $k_{ub\text{-}2} = k_{ub\text{-}1}/5\, min^{-1}$ since ubiquitination by Mdm2-P is less efficient than ubiquitination by Mdm2 [45], whereas more stable p53-2 is targeted for ubiquitination by both Mdm2 and Mdm2-P with the same rate $k_{ub\text{-}2}$. The Michaelis constant $K_{ub} = 1\, \mu M$ of the ubiquitination process is the same for both p53-1 and p53-2 ubiquitination [35]. Natural (Mdm2-independent) degradation rates for both p53-1 and p53-2 correspond to the half-life of 7 hours [33]. Natural degradation rates for Mdm2 and Mdm2-P are the same and correspond to the half-life $t_{1/2} = 30$ min according to several reports.

Since the production rate of p53-2 made from p53 mRNA bound to the complex C is 3–4-fold higher due to the active role of Mdm2-P, we consider the rate of translation $k_{tp\text{-}2}$ for p53-2 to be three times larger than the translation rate $k_{tp\text{-}1}$ for p53-1, which is equal to the translation rates for Mdm2 and Wip1 used in [16]. In the transcription process for the $Mdm2$ and $Wip1$ genes, both proteins p53-1 and p53-2 can bind DNA and stimulate gene transcription in a synergistic way in the DNA locus χ_L. Note that p53 protein is biologically active in the form of tetramers [20]. The tetramerisation of p53 molecules is not modelled explicitly, however, it is expressed by a specific choice of the Hill coefficient in the gene transciption [17, 18, 68].

Unlike [17], we include both equations for the nuclear monomeric and dimeric ATM states (denoted, respectively, by ATM-P and ATM-D). ATM dimer dissociation and monomer activation in response to DNA DSB is supposed to follow from the ATM dimer interaction with a DNA damage transmitting signal denoted by E, Figure 4. Due to a discrepancy between *in vitro* and *in vivo* experiments, E can be either the MRN complex [53] or any other signal produced by the changes in the chromatin [3]. We assume that the extent of the DNA damage can be expressed by the strength of the signal E and that ATM dimer dissociation is modelled by a Hill function with the coefficient 2.

We will also assume that all the protein species under consideration are nuclear species in the sense that they move from the translation sites in the cytoplasm (outside the ER) to the nucleus and not the other way round. On the other hand, mRNAs and the complex C move from the nucleus to the cytoplasm. For simplicity and different time scales between a molecule translocation through the nuclear membrane by the active transport mecha-

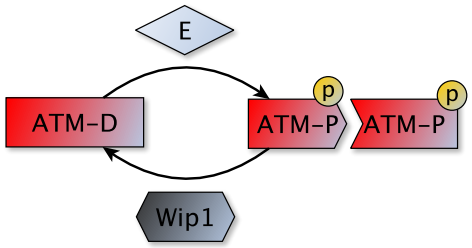

Figure 4: A schematic representation of ATM activation by a DNA-damage-transmitting substrate (although still rather hypothetical molecule) E and its deactivation by Wip1. ATM-D stands for ATM dimers and ATM-P for active ATM monomers. At each time, the total concentration is assumed to be constant $[ATM\text{-}P] + 2[ATM\text{-}D] = const =: ATM_{TOT}$.

nisms (measured in seconds or minutes) and the dynamics of proteins (measured in hours), we assume that all the translocations are based on the passive transport mechanism, are unidirectional and expressed by the so-called Kedem-Katchalsky boundary conditions (Table S1), [9, 17]. The boundary conditions are posed on the nuclear membrane and the extent of the membrane translocation is given by the translocation parameters (permeabilities). Motion of the species in the cellular compartments is assumed to be purely diffusive and we assume that the cells are homogeneous allowing the species to diffuse with the equal diffusivities over the entire compartments. The diffusions are also assumed to be unaffected by the phosphorylation status of the species. Further discussion on the diffusion and permeability issues can be found in [17, 16].

Other protein-protein interactions, e.g., phosphorylation of Mdm2 by ATM, dephosphorylation of ATM-P and Mdm2-P by Wip1, are modelled as the enzyme reactions as well. Where possible, the kinetic parameters are taken from the available literature. The missing ones are tuned by hand so that the simulations can reproduce known experimental observations. A reaction-diffusion system for the p53 dynamics with some details on the numerical method is further described in SI. Degradation rates are listed in Table S2, diffusion and permeability rates in Table S3, other kinetic parameters in Table S4.

2.3. Overview of other p53 models

Several theoretical models have been proposed to reproduce and explain the p53 oscillatory response to DNA damage at the level of single cells. Most of them used a deterministic approach based on Ordinary Differential Equations (ODE). For example, A. Ciliberto *et al.* [14] studied the negative feedback $p53 \to Mdm2 \dashv p53$ supplemented by a positive feedback involving PTEN and Akt proteins. T. Zhang *et al.* [73] explored the mechanism of [14] and proposed three other models combining the p53-Mdm2 negative feedback with three other positive feedbacks. In fact, there exist several positive feedbacks between p53 and, e.g., PTEN, p14/19 ARF, Rb, Dapk1, c-Ha-Ras, DDR1 and Rorα [24] which could, in principle, generate p53 oscillations. X.-P. Zhang *et al.* [75] used the results of [14, 73] and developed a two-phase switch model including the p53-Mdm2, ATM-p53-Wip1 and p53-PTEN-Akt-Mdm2 feedback loops to simulate irreversible transitions from cell cycle arrest to apoptosis.

An ODE model proposed by R. Lev Bar-Or *et al.* [37] and models of G. Lahav *et al.* [6, 22] were developed in order to validate the experimentally observed damped and sustained p53 oscillations, respectively. Except for p53 and Mdm2 proteins, the model in [6] includes a DNA damage signal ATM and ATM's inhibitor Wip1 (both ATM and Wip1 were experimentally identified in [6] as necessary factors for *in vitro* oscillations). The model [6] was based on Delayed Differential Equations (DDE). However, DDE models may generate artificial rhythms in systems, which do not appear naturally [32], so the biological significance of the introduced delays in the modelling protein networks can be far from obvious in those DDE models. Avoiding DDEs, the system [6] was transformed into a system of ODEs in [32] which gave oscillations thanks to a positive feedback involving Rorα.

L. Ma *et al.* [43, 67] also used DDEs to simulate particular delays in the transcription process of Mdm2 mRNA and translation of the mRNA into the protein. In our approach, physiological delays in a gene synthesis are obtained by the active (diffusive) migration of the species inside the cell (between the nucleus and the cytoplasm). Apart from our PDE models, M. Sturrock *et al.* [61, 62] and L. Dimitrio *et al.* [15] studied the sole p53-Mdm2 negative feedback in maintaining oscillatory p53 dynamics using spatio-temporal models; however, the present approach is different in the molecular background as discussed in the previous sections.

Other models include stochastic approaches by introducing either stochastic fluctuations in the protein production terms [22] or stochastic effects at the

level of transcriptional regulation and damage induction and repair [56, 52], as well as a logical approach [1].

3. Results

3.1. Dual function of Mdm2 towards p53 provides a mechanism for p53 oscillatory response

The previously described molecular mechanism based on the positive and negative regulation of p53 by Mdm2 can reproduce *in silico* the behaviour of p53 in agreement with some known experimental observations.

Indeed, Figure 5(a) shows sustained oscillations in the (nondimensionalised; adim) nuclear concentration of p53 protein (as a sum of the nuclear concentrations of p53-1 and p53-2) as well as oscillations of the other species. In response to DNA damage we see rapid ATM activation as it was observed in *in vivo* experiments [3]. The concentration of p53 then increases and peaks at the 2.4 hour time point after initiation of the DDR which corresponds to the time point observed in several experiments [6, 11, 25, 31, 37]. Another pulse reaches its maximum at $8.6\,hrs$ which is similar to the time point in real data [6, 37]. All the other oscillations reach their maxima within the period of 5.8 hours which lies in the range of observed periods [22]. A fraction of p53 (p53-1 and p53-2) that is transcriptionally active, i.e., localised in the DNA locus χ_L, is indicated by the green dashed line in Fig. 5(a). Obtained sustained oscillations are confirmed by a limit cycle in the phase plane "p53-Mdm2" plotted in Fig. 5(b). Further, after a transient decay, the concentration of Mdm2 starts to grow approximately at 1.5 hour in the DDR and peaks 4 hours after the damage, first in the cytoplasm, then in the nucleus with a time delay about 40 minutes, Fig. 5(c). Then Mdm2 reaches its basal level at the 8 hour time point similarly to several experimental data [6, 11, 25, 31, 37]. Figure 5(d) shows the total intracellular concentration of p53 mRNA either bound to the complex C or free (unbound to C) mRNA with an approximately 2.5 times difference in their concentrations. The total amount of p53 mRNA remains fairly unchanged in the DDR.

Figure 6 shows that the half-life of p53 in the cell in the presence of Mdm2 is 15 and 20 minutes when estimated from the first and second (and other) pulse, respectively, which confirms the fact that p53 is a short-lived protein [2].

2D visualisation (6 samples) of the solution of the system is shown in Figures 7 and 8. The samples are taken at the initial state and at 5 time

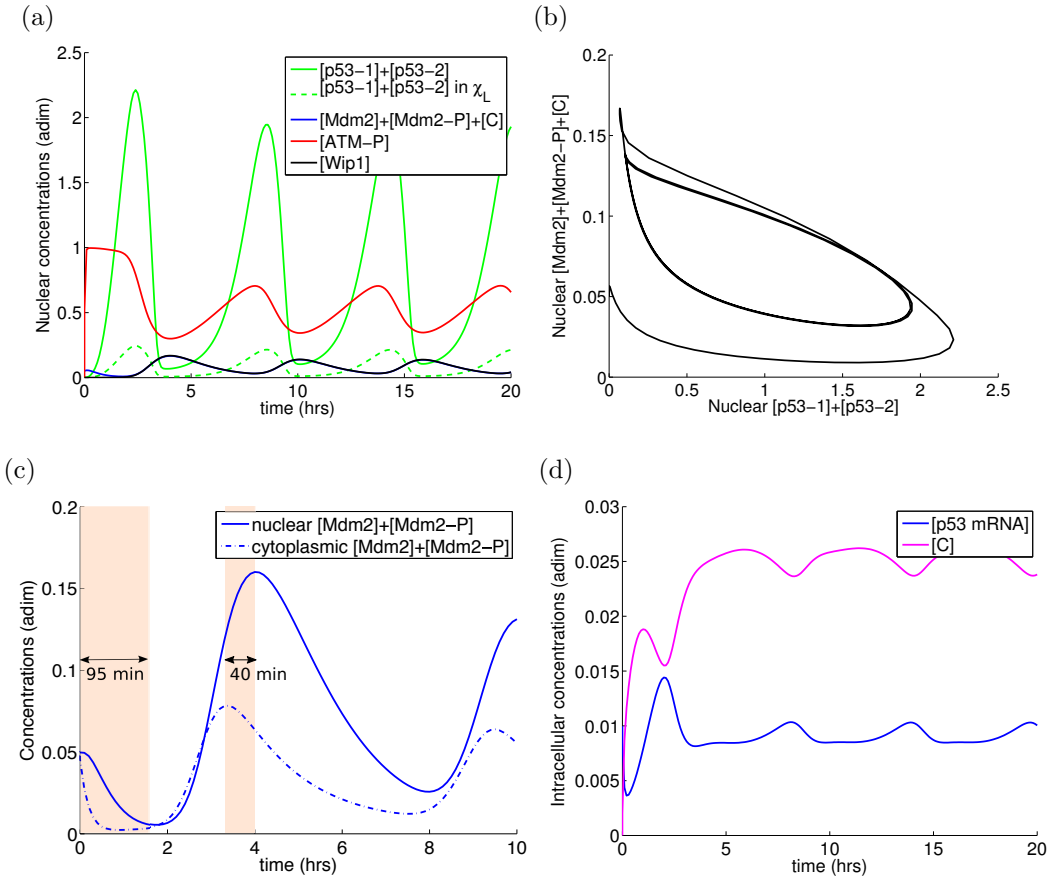

Figure 5: The solution of the RD system (see SI) in the 20 hrs time span of DDR in response to the stress signal $E = 1$ for the fixed set of parameters in Tables S2-S4. (a) Nondimensionalised (adim) nuclear concentrations of p53 (p53-1 and p53-2), Mdm2 (Mdm2, and Mdm2-P), ATM-P and Wip1; green dashed line shows the concentration of transcriptionally active p53 occurring in the DNA locus χ_L. (b) Trajectories in the phase plane (nuclear [p53], nuclear [Mdm2]). (c) Nondimensionalised (adim) nuclear and cytoplasmic concentration of Mdm2 (Mdm2 and Mdm2-P). (d) Nondimensionalised (adim) cellular "free" p53 mRNA and p53 mRNA bound to the complex C. *In these and the following graphs, the plotted concentrations are the total concentrations of the species in the cell or in a cellular compartment (see SI for more details).*

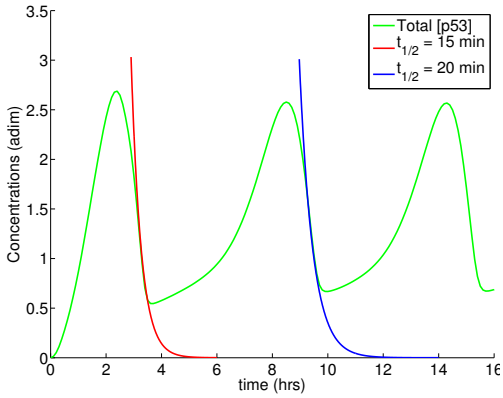

Figure 6: Decay of the cellular p53 (p53-1 and p53-2) concentration in the cell with Mdm2 in the system which corresponds to the half-life of 15 and 20 minutes, respectively, in the first and the second (and other) pulses.

points where either p53 or Mdm2 attains maximum in the concentration. Note that the values of the isolines show the range of concentrations that can be reached at each (space) point in the cell. We can also see that the concentrations of the proteins are spatially homogeneous which is caused by the diffusive dispersion of the proteins in the homogeneous medium. This is clearly unrealistic, however, note that some real samples from immunofluorescence analysis show proteins spread almost across the whole nucleus, see for example Fig. 2 (C and D) in [12] or Figures 5 and 6 in [48].

3.2. Mdm2's positive regulation of p53 is required for sustained oscillations

The enhanced translation from p53 mRNA bound to the complex C is necessary for oscillations. If we either do not allow the p53 mRNA–Mdm2-P complex formation (the association constant k_a is set to zero) or $k_a > 0$ remains as reported in Table S4 but the translation rates for both p53-1 and p53-2 are the same (i.e., $k_{tp\text{-}2} = k_{tp\text{-}1} = 1\,min^{-1}$), then we lose sustained oscillations. Instead, in both cases we observe convergence to a steady-state Figure 9: fast convergence in the former case ($k_a = 0$), Fig. 9(a) and (b), and damped oscillations in the p53 concentration in the latter case (i.e., when $k_{tp\text{-}2} = k_{tp\text{-}1}$), Fig. 9(c) and (d). Sustained oscillations can be retrieved for $k_{tp\text{-}2} \geq 1.4\,min^{-1}$ and they are still observed for values of $k_{tp\text{-}2}$ as big as $500\,min^{-1}$. Interestingly, for high values of $k_{tp\text{-}2}$ the differences between the maxima in the p53 and Mdm2 nuclear levels are of several orders of

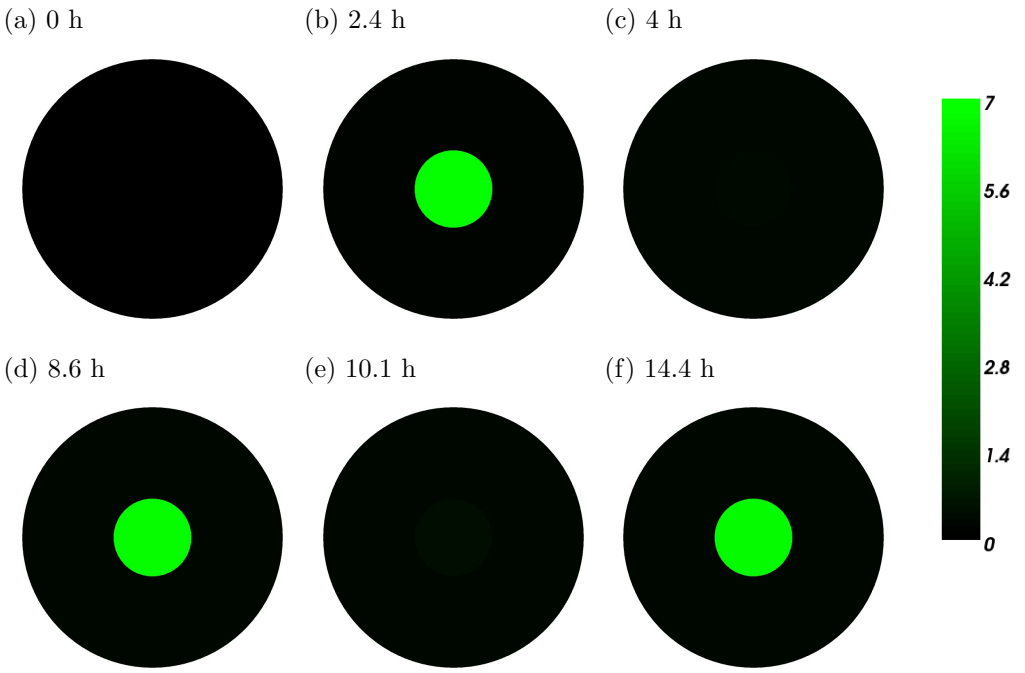

Figure 7: 2D visualisation of the solution of the RD system (see SI) with the parameters in Tables S2-S4 in a 2D cell shown in Fig. 3: samples of the nondimensionalised concentration of p53 (p53-1 and p53-2) captured at 6 time points when p53 and Mdm2 reach peaks in their concentration.

magnitude, which confirms the fact that a low concentration of Mdm2 can efficiently remove p53 from the nucleus [25].

Decreased ability of Mdm2 to target p53-2 synthesised from C for degradation or, in other words, the increased stability of p53-2 compared to the hyperunstable p53-1 protein, is necessary for sustained oscillations as well. The admissible rates $k_{ub\text{-}2}$ for the Mdm2-dependent ubiquitination of p53-2 still possessing sustained oscillations are in the range $0.02 - 3.5$ min^{-1} which is less than the reported turnover rate $k_{ub\text{-}1} = 5\,min^{-1}$ used in the ubiquitination of p53-1.

3.3. Amplitude and periods of oscillations are independent of high damage doses

It follows from single cell experiments that the amplitudes and periods of p53 oscillations are independent of the damage dose of γ-radiation or drugs

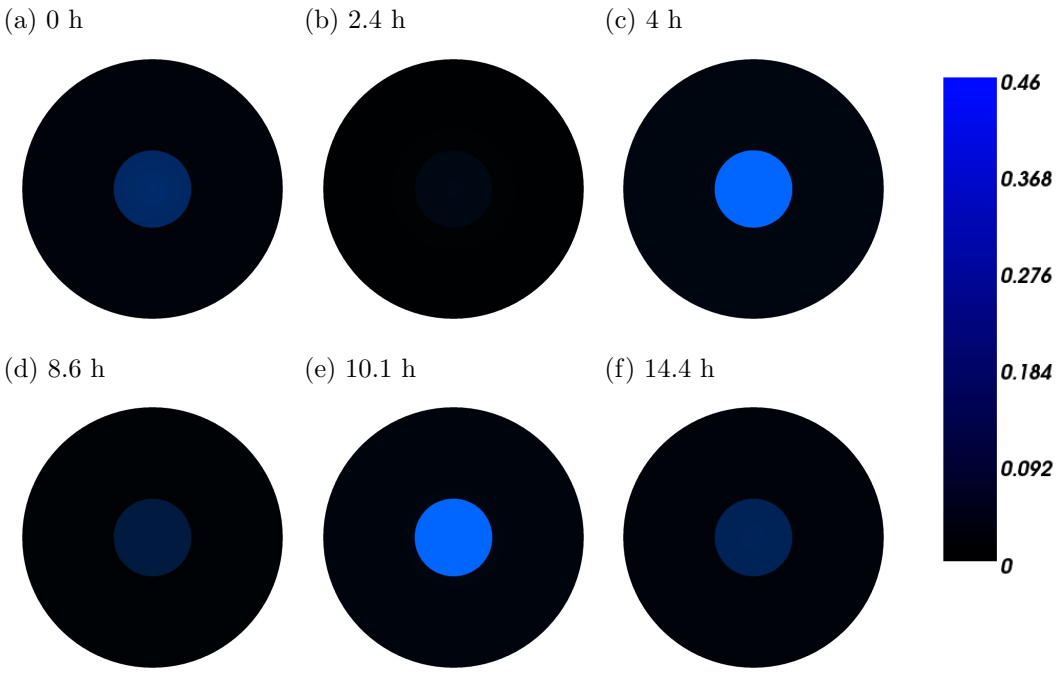

Figure 8: 2D visualisation of the solution of the RD system (see SI) with the parameters in Tables S2-S4 in a 2D cell shown in Fig. 3: samples of the nondimensionalised concentration of Mdm2 (Mdm2, Mdm2-P and C) captured at 6 time points when p53 and Mdm2 reach peaks in their concentration.

causing DSB, [22, 55].

Figure 10 shows dependence of the p53 concentration on the stress signal E starting at $E = 0$ (normal conditions) where the concentrations of the species converge to their respective steady states, Fig. 10(a). The dynamics of p53 changes from the 'convergence to the equilibrium' to the 'convergence to a (stable) limit cycle' with increasing E by passing through a bifurcation point $E_1 = 0.011$, Figure 10(b). The amplitudes and periods of the limit cycles do not change for $E > 0.25$ confirming that they are independent of the high DNA damage stimulus. Note again on this place that the DNA damage transmitting signal E is understood here as a hypothetical molecule and that further experiments have to be done to clarify the meaning of E as it is used in the model.

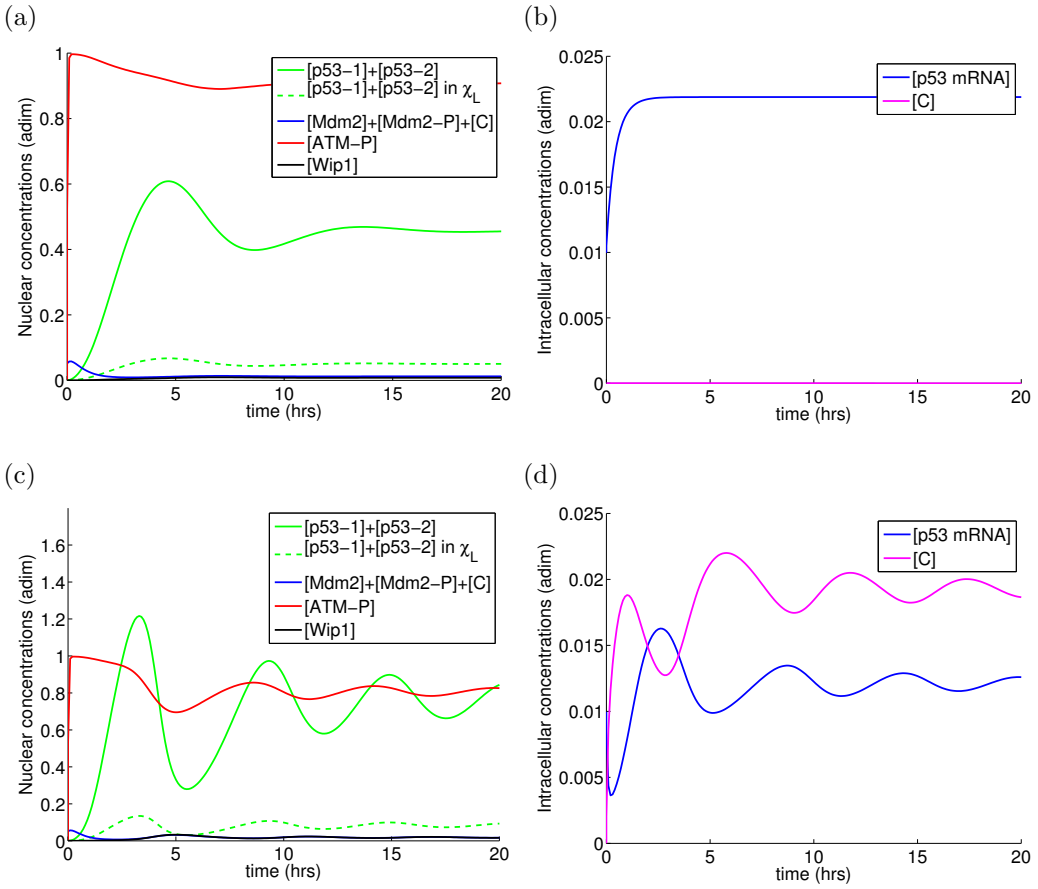

Figure 9: The solution of the RD system (see SI) in the 20 hrs time span of DDR in response to the stress signal $E = 1$ in the case when (a) and (b) Mdm2-P binding to p53 mRNA is inhibited (i.e., $k_a = 0$), (c) and (d) translation rates for p53-1 and p53-2 are the same, i.e., $k_{tp\text{-}1} = k_{tp\text{-}2} = 1\, min^{-1}$. The remaining parameters are in Tables S2-S4.

3.4. The p53 network is excitable

As discussed in the introduction, the network of p53 is excitable in response to DSB.

Inhibition of the ATM pulse one hour after DNA damage in the RD system with the parameters in Tables S2-S4 and initial and boundary conditions as described in SI reveals that the p53 model is excitable. Indeed, Figure 11(a) shows one full p53 pulse in the case when ATM-P signalling is

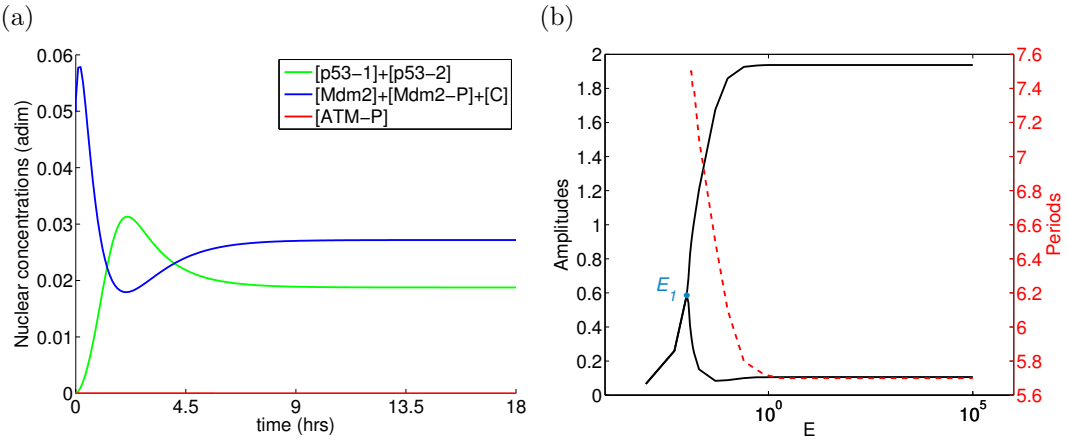

Figure 10: (a) The solution of the RD system (see SI) in the 18 hrs time span in normal conditions, $E = 0$. (b) Bifurcation diagram for the nuclear p53 concentration (p53-1 and p53-2) with respect to the varying signal E (plotted in the logarithmic scale). The bifurcation point E_1 is the point on the black curve where the curve bifurcates into two paths. The curve for $E < E_1$ shows attained steady states and plotted two curves for $E > E_1$ are the heights (showing maximum and minimum) of the amplitudes of stable limit cycles. The red dashed curve shows periods of oscillations depending on E. The parameter values used are in Tables S2-S4.

inhibited 1 hour after damage (1 hour after damage, the equation for ATM-P is "removed" from the system, which can simulate ATM-P inhibition by wortmannin). Figure 11(b) shows a full p53 pulse when ATM-P signalling is gradually silenced by Wip1 (the DNA damaging signal E is "turned off" one hour after the damage). A high amplitude excursion of the p53 concentration from a steady state followed by return to the steady state can be seen in Figure S4. These figures confirm that the response of p53 to DNA damage is excitable and independent of the input duration [40].

4. Discussion

4.1. Feedback loops between the antagonist behind the oscillator

We have shown that depending on the phosphorylation status of Mdm2, Mdm2's dual positive and negative regulation of p53 can create a p53 oscillator. The oscillator is based on our previous model [17] which is extended here

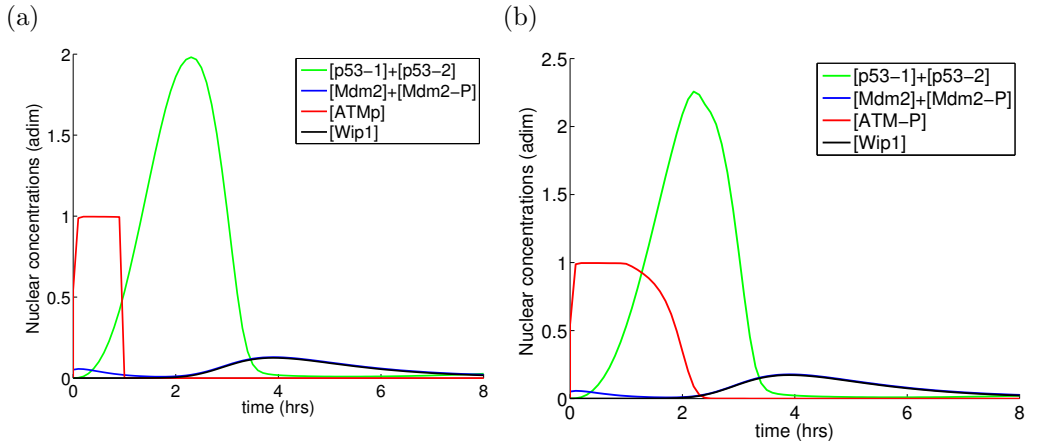

Figure 11: The solution of the RD system (see SI) where, (a), ATM-P signalling is inhibited 1 hour after damage and, (b), the damage-transmitting signal E is inhibited after one hour. The plotted concentrations are the total concentrations in the nucleus.

with a positive effect of Mdm2 on p53 expression. The two negative feedback loops used in the previous model [17] involve the classical one between p53 and Mdm2 (shortly written as $p53 \to Mdm2 \dashv p53$) and a loop between ATM and Wip1 with the intermediate p53 (i.e., $ATM\text{-}P \to p53 \to Wip1 \dashv ATM\text{-}P$), in which phosphorylation of p53 by ATM brings a stabilising effect in the p53 signalling allowing p53 to accumulate in the nucleus. Wip1 then negatively regulates ATM as well as it promotes dephosphorylation of p53 [58] and thus it closes the loop, see Figure S5(a).

In the new model, we keep the first negative feedback loop $p53 \to Mdm2 \dashv p53$, however, the second one is modified by introducing another intermediate substrate Mdm2. The loop becomes now $ATM\text{-}P \to Mdm2 \to p53 \to Wip1 \dashv ATM\text{-}P$, as shown in Figure S5(b), and we have excluded phosphorylation of p53 by ATM. Mdm2 involved in the second loop changes significantly effects of both negative feedbacks. Depending on the phosphorylation status of Mdm2, when Mdm2 is phosphorylated by ATM, then the first negative loop is weakened since Mdm2-P does not target p53 sufficiently for degradation and the second one is strengthened since Mdm2-P positively stimulates p53 synthesis yielding more stable p53 for a longer period of time. If Mdm2 is not phosphorylated by ATM, then the first negative loop is strengthened

since Mdm2 targets p53 for degradation more efficiently and the second loop is weakened since the non-phosphorylated Mdm2 cannot bind to p53 mRNA and thus it does not contribute to its synthesis by the way discussed above. Taking this together, a new mechanism of positive regulation of p53 by its dominant negative regulator Mdm2 is able to produce *in silico* sustained p53 oscillations in response to DNA damage.

4.2. Possible mechanism for the excitable response of p53

It is proposed in [5] that a possible mechanism behind the excitability of the p53 network relies likely on the fast removal of p53 inhibitors, such as Mdm2. Indeed, following phosphorylation by ATM [45], Mdm2 is observed to be rapidly degraded in response to NCS [59, 5]. The excitability could be possibly caused by a fast positive feedback which, for instance, inhibits interaction of p53 with its negative regulators (Mdm2 and Wip1) or sequesters them in the cytoplasm. This hypothesis is disfavoured in [5] by pointing out that all known positive feedbacks in the p53 response to DSB depend on the transcriptional activity of p53 (see also [24]). Thus none of them should be fast enough to excite a p53 pulse.

The experimental results in [21, 44] do not confirm any degradation of Mdm2 after phosphorylation by ATM following DNA damage as it is observed in [59, 5]. On the other hand, such phosphorylation events resulted in a positive effect of Mdm2 in the enhanced p53 synthesis [21, 44]. Our simulations suggest that the increased stability of p53 mRNA and the enhanced synthesis of more stable p53 from the mRNA bound to the complexes with Mdm2-P may serve as a "long-term source" (reservoir) of the p53 protein independently of the signalling of ATM. The excitable mechanism is thus directly dependent on the phosphorylation status of Mdm2 and the ability of Mdm2-P to bind the nascent p53 mRNA. We speculate that rather than the fast removal of Mdm2 from the site of p53 action by some positive feedback, an ATM-dependent redirection of Mdm2 from one object of interest to another, that is from targeting p53 for degradation to targeting p53 mRNA for enhanced synthesis of more stable copies of p53, can be sufficient to excite a full p53 pulse.

The dynamics of p53 in this model is similar to the dynamics of p53 from the previous model [17] where zero initial conditions for all species were assumed. However, the model in [17] does not excite any p53 pulse in response to DNA damage, see Figure S6(b). The model in [17] does not include either Mdm2 as a positive regulator of p53 or any fast removal of Mdm2-P from the

sites of p53 action. In fact, due to the initial concentration of Mdm2 there is nothing to be degraded or removed in [17]. The slope of the p53 accumulation is similar in both models (Fig 11(a) and Fig. S6(b)) in the first hour of the protein signalling. However, when ATM-P is completely inhibited, p53 continues to grow in the new model, Fig. 11(a), while the p53 level immediately drops in the old model, Fig. S6(b). Note that in the new model we do not consider any enhanced degradation of Mdm2-P either, however, we still observe decay in the Mdm2 (including phosphorylated Mdm2-P) concentration in the first hour and half, Fig. 5(c), only due to natural degradation of the protein corresponding to its half-life and because new Mdm2 molecules are pumped to the system dependently on the p53 nuclear accumulation and activity.

However, the elevated degradation of phosphorylated Mdm2 by ATM, as observed in [59, 5], can still be a realistic scenario contributing to the robustness of the p53 excitability. We can speculate that it is MdmX, which was excluded from our simulations, that determines the fate of Mdm2. If p53 mRNA–MdmX-P fails in the attraction of Mdm2-P to the complex, then Mdm2-P can be degraded through the increased self-ubiquitination. If Mdm2-P is attracted to the complex, then it can be protected against degradation and, in fact, Mdm2-P can stimulate p53 expression. The robustness can be then achieved if both events occur at the same time, that is if some Mdm2-P molecules are attracted to the complex and those Mdm2-P molecules, which are not and can ubiquitinate p53 for degradation, are themselves degraded.

The Mdm2's residue Ser395 is crucial in the binding of Mdm2-P to p53 mRNA and thus in the positive regulation of p53 expression [21, 44]. This suggests that the absent excitability in the cells exposed to UV-radiation can be (partially) explained by missing phosphorylation of this site by ATR. Indeed, ATR phosphorylates Mdm2 at Ser407 instead of Ser395 in response to UV-radiation, see for example [29] and citations therein. Further, the experiments in [5] in which Ser395 is mutated into Ser395A (disabling this residue to be phosphorylated) result in the reduced percentage of the cells that show an excitable p53 pulse. Thus we can speculate that it is phosphorylation of Mdm2's Ser395 that is important for the excitability of p53 observed in response to DNA DSB but not to DNA SSB.

All these hypotheses need to be, however, verified by further biological experiments; for example, experiments clarifying the precise role of MdmX in the degradation process of Mdm2 or experiments focused on the positive

regulation of p53 by Mdm2 in cells exposed to UV-radiation and SSB as they are done in the case of DSB in [21, 44]. Negative results of the latter experiments would support our mechanism for the excitability of p53. Note that the excitability is not seen in the case when the p53 mRNA–Mdm2-P complexes are not produced in our model, see Figure S6(a). In fact, the concentration of p53 is slowly decreasing after ATM inhibition and resembles the response to UV-radiation, see also Fig. S2(b).

The excitable p53 network is similar to the excitable neuronal systems. Due to the overall complexity of our model, it is however impossible to compare qualitatively this model with the well-known models for pulse propagation in the nerve cells, e.g., Hodgkin–Huxley or Fitzhugh–Nagumo, see [54] and citations therein. Further questions immediately arise, for example, interpretation and identification of a refractory period of time between two p53 pulses during which, roughly speaking, nothing can happen, if there is such a period at all.

Acknowledgements

The author would like to thank Jean Clairambault and Robin Fåhraeus for helpful suggestions and fruitful discussions, as well as he is grateful to the referees for their constructive input. This work was partially supported by a public grant as part of the Investissement d'avenir project, reference ANR-11-LABX-0056-LMH, LabEx LMH.

References

[1] W. Abou-Jaoudé, D. A. Ouattara, and M. Kaufman. From structure to dynamics: Frequency tuning in the p53–Mdm2 network: I. logical approach. *Journal of Theoretical Biology*, 258(4):561–577, 2009.

[2] B. Alberts, A. Johnson, J. Lewis, M. Raff, K. Roberts, and P. Walter. *Molecular Biology of the Cell. Garland Science*. Taylor and Francis Group, fifth edition, 2008.

[3] C. J. Bakkenist and M. B. Kastan. DNA damage activates ATM through intermolecular autophosphorylation and dimer dissociation through intermolecular autophosphorylation and dimer dissociation. *Nature*, 421(6922):499–506, 2003.

[4] Y. Barak, T. Juven, R. Haffner, and M. Oren. mdm2 expression is induced by wild type p53 activity. *The EMBO Journal*, 12(2):461–468, 1993.

[5] E. Batchelor, A. Loewer, C. Mock, and G. Lahav. Stimulus-dependent dynamics of p53 in single cells. *Molecular Systems Biology*, 7(1):8 pp, 2011.

[6] E. Batchelor, C. S. Mock, I. Bhan, A. Loewer, and G. Lahav. Recurrent initiation: A mechanism for triggering p53 pulses in response to DNA damage. *Molecular Cell*, 30(3):277–289, 2008.

[7] S. Ben-Tabou de Leon and E. H. Davidson. Modeling the dynamics of transcriptional gene regulatory networks for animal development. *Developmental Biology*, 325(2):317–328, 2009.

[8] J. Braga, J. G. McNally, and M. Carmo-Fonseca. A reaction-diffusion model to study RNA motion by quantitative fluorescence recovery after photobleaching. *Biophysical Journal*, 92(8):2694–2703, 2007.

[9] A. Cangiani and R. Natalini. A spatial model of cellular molecular trafficking including active transport along microtubules. *Journal of Theoretical Biology*, 267(4):614–625, 2010.

[10] Y. Chang, Y. Lee, T. Tejima, K. Tanaka, S. Omura, N. Heintz, Y. Mitsui, and J. Magae. mdm2 and bax, downstream mediators of the p53 response, are degraded by the ubiquitin-proteasome pathway. *Cell Growth Differ*, 9(1):79–84, 1998.

[11] C. Y. Chen, J. D. Oliner, Q. Zhan, A. J. Fornace, B. Vogelstein, and M. B. Kastan. Interactions between p53 and MDM2 in a mammalian cell cycle checkpoint pathway. *Proceedings of the National Academy of Sciences of the United States of America*, 91(7):2684–2688, 1994.

[12] S.-H. Chen, W. Forrester, and G. Lahav. Schedule-dependent interaction between anticancer treatments. *Science*, 351(6278):1204–1208, 2016.

[13] X. Chen, J. Chen, S. Gan, H. Guan, Y. Zhou, Q. Ouyang, and J. Shi. DNA damage strength modulates a bimodal switch of p53 dynamics for cell-fate control. *BMC Biology*, 11(1):1–11, 2013.

[14] A. Ciliberto, B. Novák, and J. J. Tyson. Steady states and oscillations in the p53/Mdm2 network. *Cell Cycle*, 4(3):488–493, 2005.

[15] L. Dimitrio, J. Clairambault, and R. Natalini. A spatial physiological model for p53 intracellular dynamics. *Journal of Theoretical Biology*, 316(0):9–24, 2013.

[16] J. Eliaš. *Mathematical model of the role and temporal dynamics of protein p53 after drug-induced DNA damage*. PhD thesis, Pierre and Marie Curie University, 2015.

[17] J. Eliaš, L. Dimitrio, J. Clairambault, and R. Natalini. The dynamics of p53 in single cells: physiologically based ODE and reaction–diffusion PDE models. *Physical Biology*, 11(4):045001, 2014.

[18] J. Eliaš, L. Dimitrio, J. Clairambault, and R. Natalini. The p53 protein and its molecular network: Modelling a missing link between DNA damage and cell fate. *Biochimica et Biophysica Acta (BBA) - Proteins and Proteomics*, 1844(1, Part B):232–247, 2014.

[19] M. Fiscella, H. Zhang, S. Fan, K. Sakaguchi, S. Shen, W. E. Mercer, G. F. Vande Woude, P. M. O'Connor, and E. Appella. Wip1, a novel human protein phosphatase that is induced in response to ionizing radiation in a p53-dependentmanner. *Proceedings of the National Academy of Sciences*, 94(12):6048–6053, 1997.

[20] P. N. Friedman, X. Chen, J. Bargonetti, and C. Prives. The p53 protein is an unusually shaped tetramer that binds directly to DNA. *Proc. Natl. Acad. Sci. USA*, 90(8):3319–3323, 1993.

[21] M. Gajjar, M. M. Candeias, L. Malbert-Colas, A. Mazars, J. Fujita, V. Olivares-Illana, and R. Fåhraeus. The p53 mRNA-Mdm2 interaction controls Mdm2 nuclear trafficking and is required for p53 activation following DNA damage. *Cancer Cell*, 21(1):25–35, 2012.

[22] N. Geva-Zatorsky, N. Rosenfeld, S. Itzkovitz, R. Milo, A. Sigal, E. Dekel, T. Yarnitzky, Y. Liron, P. Polak, G. Lahav, and U. Alon. Oscillations and variability in the p53 system. *Molecular Systems Biology*, 2(1):1–13, 2006.

[23] D. A. Hamstra, M. S. Bhojani, L. B. Griffin, B. Laxman, B. D. Ross, and A. Rehemtulla. Real-time evaluation of p53 oscillatory behavior in vivo using bioluminescent imaging. *Cancer Research*, 66(15):7482–7489, 2006.

[24] S. L. Harris and A. J. Levine. The p53 pathway: positive and negative feedback loops. *Oncogene*, 24(17):2899–2908, 2005.

[25] Y. Haupt, R. Maya, A. Kazaz, and M. Oren. Mdm2 promotes the rapid degradation of p53. *Nature*, 387(6630):296–299, 1997.

[26] F. Hecht. New development in FreeFem++. *Journal of Numerical Mathematics*, 20(3-4):251–265, 2012.

[27] P. Hinow, C. E. Rogers, C. E. Barbieri, J. A. Pietenpol, A. K. Kenworthy, and E. DiBenedetto. The DNA binding activity of p53 displays reaction-diffusion kinetics. *Biophysical Journal*, 91(1):330–342, 2006.

[28] S. Hong, Y.-N. Wang, H. Yamaguchi, H. Sreenivasappa, C.-K. Chou, P.-H. Tsou, M.-C. Hung, and J. Kameoka. Measurement of protein 53 diffusion coefficient in live hela cells using raster image correlation spectroscopy (rics). *Journal of Biomaterials and Nanobiotechnology*, 1(1):31–36, 2010.

[29] W. Hu, Z. Feng, and A. J. Levine. The regulation of multiple p53 stress responses is mediated through MDM2. *Genes & Cancer*, 3(3-4):199–208, 2012.

[30] J. Keener and J. Sneyd. *Mathematical Physiology I: Cellular Physiology*. Interdisciplinary Applied Mathematics. Springer, second edition, 2009.

[31] S. Khan, C. Guevara, G. Fujii, and D. Parry. p14ARF is a component of the p53 response following ionizing irradiation of normal human fibroblasts. *Oncogene*, 23(36):6040–6046, 2004.

[32] J. K. Kim and T. L. Jackson. Mechanisms that enhance sustainability of p53 pulses. *PloS*, 8(6):e65242, 2013.

[33] M. H. G. Kubbutat, S. N. Jones, and K. H. Vousden. Regulation of p53 stability by Mdm2. *Nature*, 387(6630):299–303, 1997.

[34] G. Lahav, N. Rosenfeld, A. Sigal, N. Geva-Zatorsky, A. J. Levine, M. B. Elowitz, and U. Alon. Dynamics of the p53-Mdm2 feedback loop in individual cells. *Nat Genet*, 36(2):147–150, 2004.

[35] Z. Lai, K. V. Ferry, M. A. Diamond, K. E. Wee, Y. B. Kim, J. Ma, T. Yang, P. A. Benfield, R. A. Copeland, and K. R. Auger. Human mdm2 mediates multiple mono-ubiquitination of p53 by a mechanism requiring enzyme isomerization. *Journal of Biological Chemistry*, 276(33):31357–31367, 2001.

[36] S. Lain and D. Lane. Improving cancer therapy by non-genotoxic activation of p53. *European Journal of Cancer*, 39(8):1053–1060, 2003.

[37] R. Lev Bar-Or, R. Maya, L. A. Segel, U. Alon, A. J. Levine, and M. Oren. Generation of oscillations by the p53-Mdm2 feedback loop: A theoretical and experimental study. *Proceedings of the National Academy of Sciences*, 97(21):11250–11255, 2000.

[38] A. J. Levine. The paths to death and differentiation. *Cell Death & Differentiation*, 18(9):1391–1392, 2011.

[39] M. Li, C. L. Brooks, F. Wu-Baer, D. Chen, R. Baer, and W. Gu. Mono- versus polyubiquitination: differential control of p53 fate by Mdm2. *Science*, 302(5652):1972–1975, 2003.

[40] A. Loewer, E. Batchelor, G. Gaglia, and G. Lahav. Basal dynamics of p53 reveal transcriptionally attenuated pulses in cycling cells. *Cell*, 142(1):89–100, 2010.

[41] A. Loewer, K. Karanam, C. Mock, and G. Lahav. The p53 response in single cells is linearly correlated to the number of DNA breaks without a distinct threshold. *BMC Biology*, 11(114):13, 2013.

[42] X. Lu, T.-A. Nguyen, S.-H. Moon, Y. Darlington, M. Sommer, and L. A. Donehower. The type 2C phosphatase Wip1: An oncogenic regulator of tumor suppressor and DNA damage response pathways. *Cancer Metastasis Reviews*, 27(2):123–135, 2008.

[43] L. Ma, J. Wagner, J. J. Rice, W. Hu, A. J. Levine, and G. A. Stolovitzky. A plausible model for the digital response of p53 to DNA damage. *Proc. Natl. Acad. Sci. USA*, 102(40):14266–14271, 2005.

[44] L. Malbert-Colas, A. Ponnuswamy, V. Olivares-Illana, A.-S. Tournillon, N. Naski, and R. Fåhraeus. HDMX folds the nascent p53 mRNA following activation by the ATM kinase. *Molecular Cell*, 54(3):500–511, 2014.

[45] R. Maya, M. Balass, S.-T. Kim, D. Shkedy, J.-F. M. Leal, O. Shifman, M. Moas, T. Buschmann, Z. Ronai, Y. Shiloh, M. B. Kastan, E. Katzir, and M. Oren. ATM-dependent phosphorylation of Mdm2 on serine 395: role in p53 activation by DNA damage. *Genes & Development*, 15(9):1067–1077, 2001.

[46] B. D. Melanson, R. Bose, J. D. Hamill, K. A. Marcellus, E. F. Pan, and B. C. McKay. The role of mRNA decay in p53-induced gene expression. *RNA*, 17(12):2222–2234, 2011.

[47] D. Michael and M. Oren. The p53–Mdm2 module and the ubiquitin system. *Seminars in Cancer Biology*, 13(1):49–58, 2003.

[48] R. Mirzayans, B. Andrais, A. Scott, and D. Murray. New insights into p53 signaling and cancer cell response to dna damage: implications for cancer therapy. *BioMed Research International*, 2012:16 pp, 2012.

[49] J. Momand, G. P. Zambetti, D. C. Olson, D. George, and A. J. Levine. The mdm-2 oncogene product forms a complex with the p53 protein and inhibits p53-mediated transactivation. *Cell*, 69(7):1237–1245, 1992.

[50] J. D. Oliner, J. A. Pietenpol, S. Thiagalingam, J. Gyuris, K. W. Kinzler, and B. Vogelstein. Oncoprotein MDM2 conceals the activation domain of tumour suppressor p53. *Nature*, 362(6423):857–860, 1993.

[51] D. C. Olson, V. Marechal, J. Momand, J. Chen, C. Romocki, and A. Levine. Identification and characterization of multiple mdm-2 proteins and mdm-2-p53 protein complexes. *Oncogene*, 8(9):2353–2360, 1993.

[52] D. A. Ouattara, W. Abou-Jaoudé, and M. Kaufman. From structure to dynamics: Frequency tuning in the p53-Mdm2 network. II: Differential and stochastic approaches. *Journal of Theoretical Biology*, 264(4):1177–1189, 2010.

[53] T. T. Paull and J.-H. Lee. The Mre11/Rad50/Nbs1 complex and its role as a DNA double-strand break sensor for ATM. *Cell Cycle*, 4(6):737–740, 2005.

[54] B. Perthame. *Transport Equations in Biology*. Birkhäuser Basel, 2007.

[55] J. E. Purvis and G. Lahav. Encoding and decoding cellular information through signaling dynamics. *Cell*, 152(5):945–956, 2013.

[56] K. Puszyński, B. Hat, and T. Lipniacki. Oscillations and bistability in the stochastic model of p53 regulation. *Journal of Theoretical Biology*, 254(2):452–465, 2008.

[57] O. Schon, A. Friedler, M. Bycroft, S. M. Freund, and A. R. Fersht. Molecular mechanism of the interaction between MDM2 and p53. *Journal of Molecular Biology*, 323(3):491–501, 2002.

[58] S. Shreeram, O. N. Demidov, W. K. Hee, H. Yamaguchi, N. Onishi, C. Kek, O. N. Timofeev, C. Dudgeon, A. J. Fornace, C. W. Anderson, Y. Minami, E. Appella, and D. V. Bulavin. Wip1 phosphatase modulates ATM-dependent signaling pathways. *Molecular Cell*, 23(5):757–764, 2006.

[59] J. M. Stommel and G. M. Wahl. Accelerated MDM2 autodegradation induced by DNAdamage kinases is required for p53 activation. *The EMBO Journal*, 23(7):1547–1556, 2004.

[60] M. Sturrock, A. Hellander, A. Matzavinos, and M. A. J. Chaplain. Spatial stochastic modelling of the Hes1 gene regulatory network: intrinsic noise can explain heterogeneity in embryonic stem cell differentiation. *Journal of The Royal Society Interface*, 10(80):20120988, 2013.

[61] M. Sturrock, A. J. Terry, D. P. Xirodimas, A. M. Thompson, and M. A. J. Chaplain. Spatio-temporal modelling of the Hes1 and p53-Mdm2 intracellular signalling pathways. *Journal of Theoretical Biology*, 273(1):15–31, 2011.

[62] M. Sturrock, A. J. Terry, D. P. Xirodimas, A. M. Thompson, and M. A. J. Chaplain. Influence of the nuclear membrane, active transport, and cell shape on the hes1 and p53-Mdm2 pathways: insights

from spatio-temporal modelling. *Bulletin of Mathematical Biology*, 74(7):1531–1579, 2012.

[63] D. Y. Vargas, A. Raj, S. A. Marras, F. R. Kramer, and S. Tyagi. Mechanism of mRNA transport in the nucleus. *Proc. Natl. Acad. Sci. USA*, 102(47):17008–17013, 2005.

[64] B. Vogelstein, D. Lane, and A. J. Levine. Surfing the p53 network. *Nature*, 408(6810):307–310, 2000.

[65] K. H. Vousden and D. P. Lane. p53 in health and disease. *Nature Reviews: Molecular Cell Biology*, 8(4):275–283, 2007.

[66] K. H. Vousden and C. Prives. Blinded by the light: the growing complexity of p53. *Cell*, 137(3):413–431, 2009.

[67] J. Wagner, L. Ma, J. Rice, W. Hu, A. Levine, and G. Stolovitzky. p53–Mdm2 loop controlled by a balance of its feedback strength and effective dampening using ATM and delayed feedback. *IEE Proceedings-Systems Biology*, 152(3):109–118, 2005.

[68] R. L. Weinberg, D. B. Veprintsev, and A. R. Fersht. Cooperative binding of tetrameric p53 to DNA. *Journal of Molecular Biology*, 341(5):1145–1159, 2004.

[69] X. Wu, J. H. Bayle, D. Olson, and A. J. Levine. The p53-mdm-2 autoregulatory feedback loop. *Genes & Development*, 7(7a):1126–1132, 1993.

[70] H. Yamaguchi, S. R. Durell, D. K. Chatterjee, C. W. Anderson, and E. Appella. The Wip1 phosphatase PPM1D dephosphorylates SQ/TQ motifs in checkpoint substrates phosphorylated by PI3K-like kinases. *Biochemistry*, 46(44):12594–12603, 2007.

[71] Y. Yin, C. W. Stephen, M. G. Luciani, and R. Fahraeus. p53 stability and activity is regulated by Mdm2-mediated induction of alternative p53 translation products. *Nat Cell Biol*, 4(6):462–467, 2002.

[72] D. B. Young, J. Jonnalagadda, M. Gatei, D. A. Jans, S. Meyn, and K. K. Khanna. Identification of domains of ataxia-telangiectasia mutated required for nuclear localization and chromatin association. *Journal of Biological Chemistry*, 280(30):27587–27594, 2005.

[73] T. Zhang, P. Brazhnik, and J. J. Tyson. Exploring mechanisms of the DNA-damage response: p53 pulses and their possible relevance to apoptosis. *Cell Cycle*, 6(1):85–94, 2007.

[74] X. Zhang, L. Lin, H. Guo, J. Yang, S. N. Jones, A. Jochemsen, and X. Lu. Phosphorylation and degradation of MdmX is inhibited by Wip1 phosphatase in the DNA damage response. *Cancer Research*, 69(20):7960–7968, 2009.

[75] X.-P. Zhang, F. Liu, and W. Wang. Two-phase dynamics of p53 in the DNA damage response. *Proc. Natl. Acad. Sci. USA*, 108(22):8990–8995, 2011.

Suplemental Information

Reaction-diffusion system

For a simplified notation, denote the concentrations of species in their nuclear and cytoplasmic states (distinguished by the superscripts (n) and (c), respectively) by

$$\begin{aligned} u_0 = [ATM\text{-}P]^{(n)}, u_0^D = [ATM\text{-}D]^{(n)} \\ u_1 = [p53\ mRNA]^{(n)}, u_2 = [C]^{(n)}, u_3 = [p53\text{-}1]^{(n)}, u_4 = [p53\text{-}2]^{(n)}, \\ u_5 = [Wip1\ mRNA]^{(n)}, u_6 = [Wip1]^{(n)}, \\ u_7 = [Mdm2\ mRNA]^{(n)}, u_8 = [Mdm2]^{(n)}, u_9 = [Mdm2\text{-}P]^{(n)}, \end{aligned} \tag{S1}$$

and

$$\begin{aligned} v_0 = [ATM\text{-}P]^{(c)}, v_0^D = [ATM\text{-}D]^{(c)} \\ v_1 = [p53\ mRNA]^{(c)}, v_2 = [C]^{(c)}, v_3 = [p53\text{-}1]^{(c)}, v_4 = [p53\text{-}2]^{(c)}, \\ v_5 = [Wip1\ mRNA]^{(c)}, v_6 = [Wip1]^{(c)}, \\ v_7 = [Mdm2\ mRNA]^{(c)}, v_8 = [Mdm2]^{(c)}, v_9 = [Mdm2\text{-}P]^{(c)}, \end{aligned} \tag{S2}$$

where, for each i, $u_i = u_i(t, \mathbf{x})$ and $v_i = v_i(t, \mathbf{x})$ are real functions of the time $t > 0$ and the space $\mathbf{x} \in \Omega$ for a domain Ω as on Fig. S3. The diffusive motion is expressed by the Laplacian Δ. The equations for the nuclear concentrations are given by

$$\frac{\partial u_0}{\partial t} - D_{ATM}\Delta u_0 = \underbrace{2k_{ph2}u_0^D \frac{E^2}{K_{ph2}^2 + E^2}}_{\text{ATM-P activation}} - \underbrace{k_{dph2}u_6 \frac{u_0}{K_{dph2} + u_0}}_{\substack{\text{ATM-P dephosphorylation} \\ \text{by Wip1}}}$$

$$\frac{\partial u_0^D}{\partial t} - D_{ATM}\Delta u_0^D = -\underbrace{k_{ph2}u_0^D \frac{E^2}{K_{ph2}^2 + E^2}}_{\text{ATM-P activation}} + \underbrace{\frac{1}{2}k_{dph2}u_6 \frac{u_0}{K_{dph2} + u_0}}_{\substack{\text{ATM-P dephosphorylation} \\ \text{by Wip1}}}$$

$$\frac{\partial u_1}{\partial t} - D_{pRNA}\Delta u_1 = \underbrace{k_S\chi_L}_{\substack{\text{mRNA basal} \\ \text{production}}} - \underbrace{k_a u_1 u_9 \chi_L}_{\substack{\text{p53 mRNA–Mdm2-P} \\ \text{production in } \chi_L}} - \underbrace{\delta_{pRNA}u_1}_{\substack{\text{natural} \\ \text{degradation}}}$$

$$
\begin{aligned}
\frac{\partial u_2}{\partial t} - D_C \Delta u_2 &= \underbrace{k_a u_1 u_9 \chi_L}_{\substack{\text{p53 mRNA–Mdm2-P} \\ \text{production in } \chi_L}} - \underbrace{\delta_C u_2}_{\substack{\text{natural} \\ \text{degradation}}} \\
\frac{\partial u_3}{\partial t} - D_{p53} \Delta u_3 &= - \underbrace{(k_{ub\text{-}1} u_8 + k_{ub\text{-}2} u_9) \frac{u_3}{K_{ub} + u_3}}_{\substack{\text{p53-1 degradation due to} \\ \text{ubiquitination by Mdm2 and Mdm2-P}}} - \underbrace{\delta_{p53} u_3}_{\substack{\text{natural} \\ \text{degradation}}} \\
\frac{\partial u_4}{\partial t} - D_{p53} \Delta u_4 &= - \underbrace{k_{ub\text{-}2} (u_8 + u_9) \frac{u_4}{K_{ub} + u_4}}_{\substack{\text{p53-2 degradation due to} \\ \text{ubiquitination by Mdm2 and Mdm2-P}}} - \underbrace{\delta_{p53} u_4}_{\substack{\text{natural} \\ \text{degradation}}} \qquad \text{(S3)} \\
\frac{\partial u_5}{\partial t} - D_{wRNA} \Delta u_5 &= \underbrace{k_{Sw} \chi_L}_{\substack{\text{mRNA basal} \\ \text{production}}} + \underbrace{k_{S_{pw}} \frac{(u_3 + u_4)^4}{K_{S_{pw}}^4 + (u_3 + u_4)^4} \chi_L}_{\substack{\text{Wip1 mRNA transcription} \\ \text{by p53-1 and p53-2}}} - \underbrace{\delta_{wRNA} u_5}_{\substack{\text{natural} \\ \text{degradation}}} \\
\frac{\partial u_6}{\partial t} - D_{wip1} \Delta u_6 &= - \underbrace{\delta_{wip1} u_6}_{\substack{\text{natural} \\ \text{degradation}}} \\
\frac{\partial u_7}{\partial t} - D_{mRNA} \Delta u_7 &= \underbrace{k_{Sm} \chi_L}_{\substack{\text{mRNA basal} \\ \text{production}}} + \underbrace{k_{S_{pm}} \frac{(u_3 + u_4)^4}{K_{S_{pm}}^4 + (u_3 + u_4)^4} \chi_L}_{\substack{\text{Mdm2 mRNA transcription} \\ \text{by p53-1 and p53-2}}} - \underbrace{\delta_{mRNA} u_7}_{\substack{\text{natural} \\ \text{degradation}}} \\
\frac{\partial u_8}{\partial t} - D_{mdm2} \Delta u_8 &= - \underbrace{k_{ph3} u_0 \frac{u_8}{K_{ph3} + u_8}}_{\substack{\text{Mdm2 phosphorylation} \\ \text{by ATM-P}}} + \underbrace{k_{dph3} u_6 \frac{u_9}{K_{dph3} + u_9}}_{\substack{\text{Mdm2-P dephosphorylation} \\ \text{by Wip1}}} - \underbrace{\delta_{mdm2} u_8}_{\substack{\text{natural} \\ \text{degradation}}} \\
\frac{\partial u_9}{\partial t} - D_{mdm2} \Delta u_9 &= \underbrace{k_{ph3} u_0 \frac{u_8}{K_{ph3} + u_8}}_{\substack{\text{Mdm2 phosphorylation} \\ \text{by ATM-P}}} - \underbrace{k_{dph3} u_6 \frac{u_9}{K_{dph3} + u_9}}_{\substack{\text{Mdm2-P dephosphorylation} \\ \text{by Wip1}}} \\
&\quad - \underbrace{k_a u_1 u_9 \chi_L}_{\substack{\text{p53 mRNA–Mdm2-P} \\ \text{production in } \chi_L}} - \underbrace{\delta_{mdm2} u_9}_{\substack{\text{natural} \\ \text{degradation}}}
\end{aligned}
$$

while the equations for the cytoplasmic concentrations by

$$
\frac{\partial v_0}{\partial t} - D_{ATM} \Delta v_0 = 0
$$

$$
\begin{aligned}
&\frac{\partial v_0^D}{\partial t} - D_{ATM}\Delta v_0^D = 0\\
&\frac{\partial v_1}{\partial t} - D_{pRNA}\Delta v_1 = \underbrace{k_d v_2}_{\substack{\text{complex } C\\ \text{dissociation}}} - \underbrace{\delta_{pRNA} v_1}_{\substack{\text{natural}\\ \text{degradation}}}\\
&\frac{\partial v_2}{\partial t} - D_C\Delta v_2 = - \underbrace{k_d v_2}_{\substack{\text{complex } C\\ \text{dissociation}}} - \underbrace{\delta_C v_2}_{\substack{\text{natural}\\ \text{degradation}}}\\
&\frac{\partial v_3}{\partial t} - D_{p53}\Delta v_3 = \underbrace{k_{tp\text{-}1} v_1 \chi_{CD}}_{\text{mRNA translation}} - \underbrace{(k_{ub\text{-}1} v_8 + k_{ub\text{-}2} v_9)\frac{v_3}{K_{ub} + v_3}}_{\substack{\text{p53-1 degradation due to}\\ \text{ubiquitination by Mdm2 and Mdm2-P}}} - \underbrace{\delta_{p53} v_3}_{\substack{\text{natural}\\ \text{degradation}}}\\
&\frac{\partial v_4}{\partial t} - D_{p53}\Delta v_4 = \underbrace{k_{tp\text{-}2} v_2 \chi_{CD}}_{\text{mRNA translation}} - \underbrace{k_{ub\text{-}2}(v_8 + v_9)\frac{v_4}{K_{ub} + v_4}}_{\substack{\text{p53-2 degradation due to}\\ \text{ubiquitination by Mdm2 and Mdm2-P}}} - \underbrace{\delta_{p53} v_4}_{\substack{\text{natural}\\ \text{degradation}}}
\end{aligned}
\tag{S4}
$$

$$
\begin{aligned}
&\frac{\partial v_5}{\partial t} - D_{wRNA}\Delta v_5 = - \underbrace{\delta_{wRNA} v_5}_{\substack{\text{natural}\\ \text{degradation}}}\\
&\frac{\partial v_6}{\partial t} - D_{wip1}\Delta v_6 = \underbrace{k_{tw} v_5 \chi_{CD}}_{\text{mRNA translation}} - \underbrace{\delta_{wip1} v_6}_{\substack{\text{natural}\\ \text{degradation}}}\\
&\frac{\partial v_7}{\partial t} - D_{mRNA}\Delta v_7 = - \underbrace{\delta_{mRNA} v_7}_{\substack{\text{natural}\\ \text{degradation}}}\\
&\frac{\partial v_8}{\partial t} - D_{mdm2}\Delta v_8 = \underbrace{k_{tm} v_7 \chi_{CD}}_{\text{mRNA translation}} + \underbrace{k_{dph3} v_6 \frac{v_9}{K_{dph3} + v_9}}_{\substack{\text{Mdm2-P dephosphorylation}\\ \text{by Wip1}}} - \underbrace{\delta_{mdm2} v_8}_{\substack{\text{natural}\\ \text{degradation}}}\\
&\frac{\partial v_9}{\partial t} - D_{mdm2}\Delta v_9 = \underbrace{k_d v_2}_{\substack{\text{complex } C\\ \text{dissociation}}} - \underbrace{k_{dph3} v_6 \frac{v_9}{K_{dph3} + v_9}}_{\substack{\text{Mdm2-P dephosphorylation}\\ \text{by Wip1}}} - \underbrace{\delta_{mdm2} v_9}_{\substack{\text{natural}\\ \text{degradation}}}
\end{aligned}
$$

The DNA locus χ_L and the translation area χ_{CD}, as they are defined in Fig. 3, are the classical characteristic functions in the above equations (S3)-

(S4). The Kedem–Katchalsky boundary conditions on the nuclear membrane Γ_1 taking into account the assumptions on the movement of species are listed in Table S1. It is further assumed that the species cannot leave the cell, i.e., $D_i \partial_{\mathbf{n}_2} v_i = 0$ where i goes throughout all the species.

The system (S3)-(S4) is nondimensionalised in a similar way as the PDE system in [17] with the characteristic values for time $\tau = 1\,min$, length $L = 10\,\mu m$ and concentrations $\alpha_i = 1\,\mu M$ for each species i. Thus the received numerical concentrations will be adimensional (adim). The plots in figures (e.g., in Fig. 5) show the total concentrations of proteins/mRNAs in the cell or in a compartment, i.e., $\int_\Omega u_i + v_i$ or $\int_{\Omega_1} u_i$ or $\int_{\Omega_2} v_i$ for some species $i \in \{0, \ldots, 9\}$ where Ω_1 denotes the nucleus and Ω_2 denotes the cytoplasm (see Fig. S3).

We will also consider zero initial conditions for almost all species except for Mdm2 and p53 mRNA which are assumed to be 0.1 and 0.01 (adim), respectively, homogeneously distributed over the cell, i.e., we consider

$$\begin{gathered} \int u_1(0,\mathbf{x}) + v_1(0,\mathbf{x})\,\mathrm{d}x = 0.01 \quad \text{and} \quad \int u_8(0,\mathbf{x}) + v_8(0,\mathbf{x})\,\mathrm{d}x = 0.1. \\ u_i(0,\mathbf{x}) = v_i(0,\mathbf{x}) = 0, \text{ otherwise.} \end{gathered} \tag{S5}$$

The system (S3)-(S4) is solved numerically in 2D and 3D in FreeFem++ [26]. We select a uniform discretisation (consisting of 2500 elements) of the spatial domain in Figure 3. The method for calculating numerical solutions is the semi-implicit time discretisation. Then the resulting system is discretised thanks to P1 Finite Element Method. For more details and an explicitly solved problem, though a simpler problem than presented here, we refer to [16]. In figures we show 2D simulations since we do not observe dramatic differences between 2D and 3D results, as we did not observe in [17] either.

803

804 **Tables**

Substrate	Nuclear changes	Cytoplasmic changes
ATM-P	$-D_{ATM}\frac{\partial u_0}{\partial \mathbf{n}_1} = 0$	$D_{ATM}\frac{\partial v_0}{\partial \mathbf{n}_1} = 0$
ATM-D	$-D_{ATM}\frac{\partial u_0^D}{\partial \mathbf{n}_1} = 0$	$D_{ATM}\frac{\partial v_0^D}{\partial \mathbf{n}_1} = 0$
p53 mRNA	$-D_{pRNA}\frac{\partial u_1}{\partial \mathbf{n}_1} = p_{pRNA}u_1$	$D_{pRNA}\frac{\partial v_1}{\partial \mathbf{n}_1} = -p_{pRNA}u_1$
C	$-D_C\frac{\partial u_2}{\partial \mathbf{n}_1} = p_C u_2$	$D_C\frac{\partial v_2}{\partial \mathbf{n}_1} = -p_C u_2$
p53-1	$-D_{p53}\frac{\partial u_3}{\partial \mathbf{n}_1} = -p_{p53}v_3$	$D_{p53}\frac{\partial v_3}{\partial \mathbf{n}_1} = p_{p53}v_3$
p53-2	$-D_{p53}\frac{\partial u_4}{\partial \mathbf{n}_1} = -p_{p53}v_4$	$D_{p53}\frac{\partial v_4}{\partial \mathbf{n}_1} = p_{p53}v_4$
Wip1 mRNA	$-D_{wRNA}\frac{\partial u_5}{\partial \mathbf{n}_1} = p_{wRNA}u_5$	$D_{wRNA}\frac{\partial v_5}{\partial \mathbf{n}_1} = -p_{wRNA}u_5$
Wip1	$-D_{wip1}\frac{\partial u_6}{\partial \mathbf{n}_1} = -p_{wip1}v_6$	$D_{wip1}\frac{\partial v_6}{\partial \mathbf{n}_1} = p_{wip1}v_6$
Mdm2 mRNA	$-D_{mRNA}\frac{\partial u_7}{\partial \mathbf{n}_1} = p_{mRNA}u_7$	$D_{mRNA}\frac{\partial v_7}{\partial \mathbf{n}_1} = -p_{mRNA}u_7$
Mdm2	$-D_{mdm2}\frac{\partial u_8}{\partial \mathbf{n}_1} = -p_{mdm2}v_8$	$D_{mdm2}\frac{\partial v_8}{\partial \mathbf{n}_1} = p_{mdm2}v_8$
Mdm2-P	$-D_{mdm2}\frac{\partial u_9}{\partial \mathbf{n}_1} = -p_{mdm2}v_9$	$D_{mdm2}\frac{\partial v_9}{\partial \mathbf{n}_1} = p_{mdm2}v_9$

Table S1: The Kedem–Katchalsky transmission boundary conditions on Γ_1 with the diffusion D_i and translocation p_i coefficients for the RD system (S3)-(S4) modelling p53 dynamics with a dual function of Mdm2 towards p53. Whilst neither ATM dimers (ATM-D) nor ATM-P are allowed to leave the nucleus, the complex C, p53, Wip1 and Mdm2 mRNAs move from the nucleus to the cytoplasm and the proteins p53-1, p53-2, Mdm2 and Wip1 from the cytoplasm to the nucleus as well as Mdm2-P unless it is bound to C.

Substrate	$t_{1/2}$ $[h]$	$\delta = \frac{\log 2}{t_{1/2}}$ $[h^{-1}]$
p53 (with wt Mdm2)	1/3 [51]	2
p53 (without wt Mdm2)	7 [33]	0.1
p53 mRNA	1/3 [2]	2
Mdm2 mRNA	1 [46]	0.7
Wip1 mRNA*	—	0.7
C	1 [chosen]	0.7
Mdm2	0.5 [10, 51, 69]	1.38
Wip1*	—	1.38

Table S2: The half-lives $t_{1/2}$ and the corresponding degradation rates δ of the species used in the models;
*the half-lives of the Wip1 and its mRNA are not known to us, therefore we assume that they are equal to the half-lives of Mdm2 and Mdm2 mRNA.

Substrate	Diffusion $[\mu m^2/min]$	Weight $[kDa]$	Permeability $[\mu m/min]$	
GFP	—	2500 [27, 28]	26.9 [27]	—	—
p53-GFP	—	900 [27, 28]	∼80 [27]	—	—
p53	D_{p53}	1000 [27, 28]	53 [71]	p_{p53}	1 [est.]
p53 mRNP	D_{pRNA}	1.8 [8, 63]	—	p_{pRNA}	0.1 [est.]
C	D_C	1.8 [8, 63]	—	p_C	0.1 [est.]
Mdm2	D_{mdm2}	1000 [est.]	90 [49, 69]	p_{mdm2}	1 [est.]
Mdm2 mRNP	D_{mRNA}	1.8 [8, 63]	—	p_{mRNA}	0.1 [est.]
ATM	D_{ATM}	300 [est.]	370 [3]	p_{ATM}	0
Wip1	D_{wip1}	1000 [est.]	61 [19]	p_{wip1}	1 [est.]
Wip1 mRNP	D_{wRNA}	1.8 [8, 63]	—	p_{wRNA}	0.1 [est.]

Table S3: Diffusion and permeability coefficients used in the model. The diffusion rates are estimated roughly by the comparison of the known diffusions and the molecular weights of the species. We assume that mRNAs diffuse with a rate of an average mRNA-Protein (mRNP) complex, [8, 63]. Although we consider ATM in its monomeric and dimeric state we assume that both conformations diffuse with the same rate. Similarly, we assume that the diffusivities of p53-1 and p53-2 as well as Mdm2 and Mdm2-P are the same. Due to the lack of data on permeabilities, we have run several simulations and tested various permeability rates for which oscillations appear. We assume that ATM does not leave nor enter the nucleus, thus $p_{ATM} = 0$.

Parameter	Value [Units]	Description
$k_{ub\text{-}1}$	5 $[min^{-1}]$	rate of Mdm2-dependent ubiquitination of p53-1, [35]
$k_{ub\text{-}2}$	1 $[min^{-1}]$	rate of Mdm2-dependent ubiquitination of p53-2, [est.]
K_{ub}	1 $[\mu M]$	Michaelis rate of Mdm2-dependent ubiquitination of p53, [35]
k_S^*	0.0005 $[\mu M\, min^{-1} \lvert\chi_L\rvert^{-1}]$	basal synthesis rate of p53 mRNA, [est.]
$k_{tp\text{-}1}$	1 $[min^{-1}]$	translation rate for p53-1, [7]
$k_{tp\text{-}2}$	3 $[min^{-1}]$	translation rate for p53-2, [21, 44]
k_{Sm}^*	0.000005 $[\mu M\, min^{-1} \lvert\chi_L\rvert^{-1}]$	basal synthesis rate of Mdm2 mRNA, [est.]
$k_{S_{pm}}$	0.03 $[\mu M\, min^{-1}]$	velocity of Mdm2 mRNA transcription, [est.]
$K_{S_{pm}}$	10 $[\mu M]$	Michaelis rate of Mdm2 mRNA transcription, [est.]
k_{tm}	1 $[min^{-1}]$	translation rate for Mdm2, [7]
k_{Sw}^*	0.000003 $[\mu M\, min^{-1} \lvert\chi_L\rvert^{-1}]$	basal synthesis rate of Wip1 mRNA, [est.]
$k_{S_{pw}}$	0.03 $[\mu M\, min^{-1}]$	velocity of Wip1 mRNA transcription, [est.]
$K_{S_{pw}}$	10 $[\mu M]$	Michaelis rate of Wip1 mRNA transcription, [est.]
k_{tw}	1 $[min^{-1}]$	translation rate for Wip1, [7]
k_{ph2}	1 $[min^{-1}]$	velocity of ATM activation by E, [est.]
K_{ph2}	0.3 $[\mu M]$	Michaelis rate of ATM activation by E, [est.]
k_{dph2}	96 $[min^{-1}]$	rate of Wip1-dependent dephoshorylation of ATM-P, [58]
K_{dph2}	26 $[\mu M]$	Michaelis rate of Wip1-dependent dephoshorylation of ATM-P, [58]
k_{ph3}	1 $[min^{-1}]$	velocity of ATM-dependent phoshorylation of Mdm2, [est.]
K_{ph3}	1 $[\mu M]$	Michaelis rate of ATM-dependent phoshorylation of Mdm2, [est.]
k_{dph3}	84 $[min^{-1}]$	rate of Wip1-dependent dephoshorylation of Mdm2-P, [70]
K_{dph3}	23 $[\mu M]$	Michaelis rate of Wip1–dependent dephoshorylation of Mdm2-P, [70]
k_a	20 $[min^{-1}]$	association rate for the complex C, [est.]
k_d	0.01 $[\mu M^{-1}\, min^{-1}]$	dissociation rate from the complex C, [est.]
E	1 $[\mu M]$	concentration of "the damage signal", [chosen]
ATM_{TOT}	1 $[\mu M]$	total ATM concentration, [chosen]

Table S4: Parameter values for the RD system (S3)-(S4) modelling p53 dynamics with a dual function of Mdm2 toward p53. Degradation terms, diffusivities and permeabilities are shown separately in Tables S2 and S3. **The constant rates represent the total net production in a certain area of the cell, e.g., the (p53, Mdm2, Wip1) RNAs are produced with the basal rates* k_S, k_{Sm} *and* k_{Sw} *of the assigned values over the whole DNA locus* χ_L.

Figures

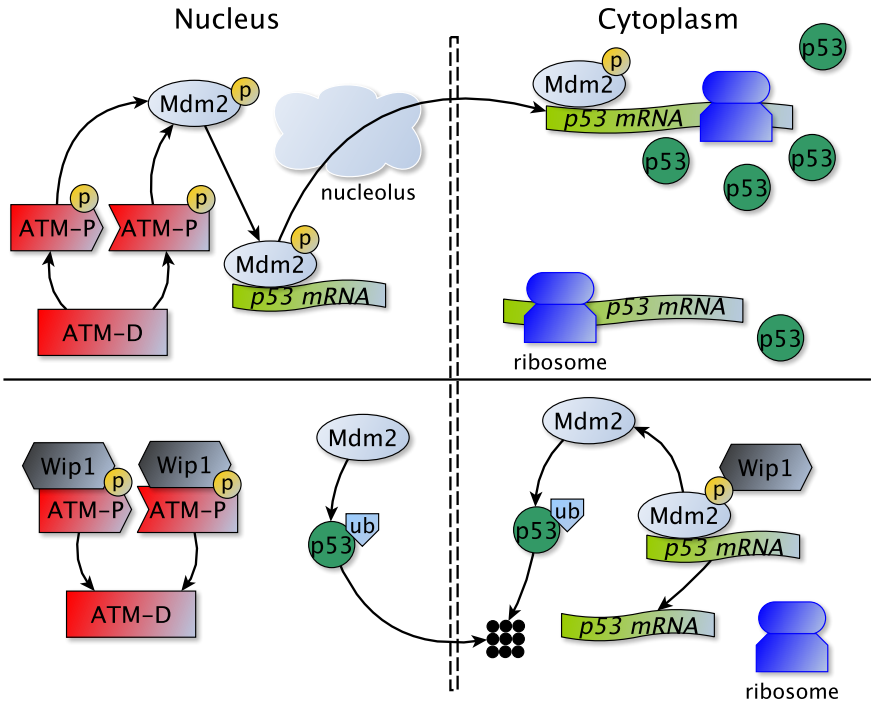

Figure S1: A simplified positive effect of Mdm2 towards p53: The molecular network remains the same as in Figure 2 except for the protein MdmX which is omitted. In the presence of DNA damage, inactive ATM dimers dissociate into active monomers [3], which phosphorylate Mdm2 at Ser395 in the nuclear compartment [3, 72]. Mdm2-P then binds to a nascent p53 mRNA at the DNA sites, assuming that the structure of mRNA has been previously modified to a form which allows this binding, and move together from the nucleus to the cytoplasm. In the cytoplasm, Mdm2-P enhances p53 translation from its mRNA and, at the same time, Mdm2-P is less capable of p53 ubiquitination. This all enables p53 to accumulate in the nucleus where it acts as a transcription factor for the *Mdm2* and *Wip1* genes [4, 19]. The phosphatase Wip1 targets ATM-P for dephosphorylation and thus inactivation [58]. Wip1 reverses also Mdm2 and MdmX phosphorylation status, [70, 74], so that Mdm2 promotes ubiquitination and degradation of p53. The persistent DNA damage signal can trigger another pulse of p53 by ATM dimer monomerisation again.

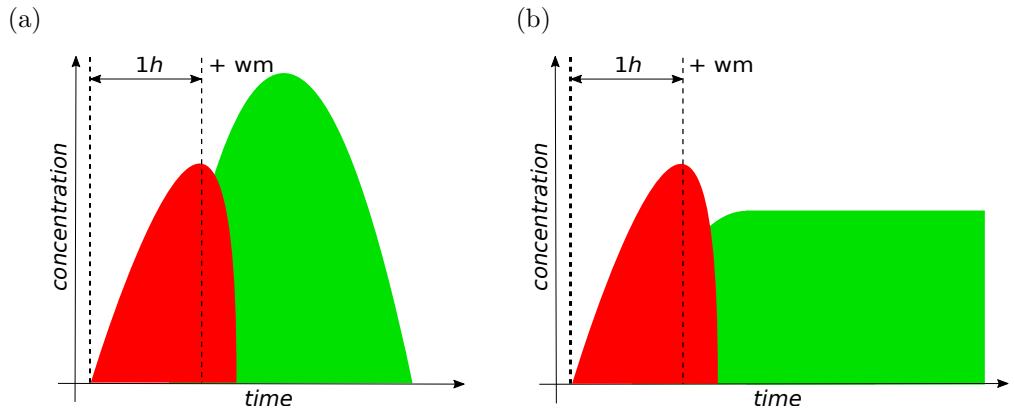

Figure S2: A schematic representation of the dynamics of p53, which (a) is excitable in response to γ-radiation or some drugs, i.e., a transient signalling of ATM (red) for one hour is sufficient to trigger one full pulse of p53 (green); (b) is not excitable in response to UV-radiation, i.e., a transient input of ATR (red) results to a rather constant p53 response (green), [5].

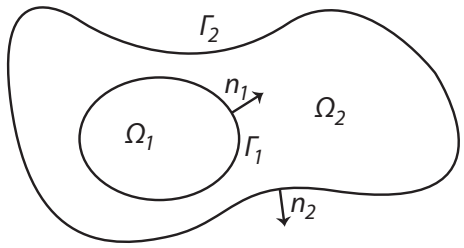

Figure S3: Cell scheme: the nucleus Ω_1, the cytoplasm Ω_2, the nuclear membrane Γ_1 and the cell membrane Γ_2; n_1 and n_2 are the unit normal vectors oriented, respectively, outward from Ω_1 and Ω_2. Note that neither the DNA locus χ_L nor the ER are separated by membranes in our model, thus we can treat them as integral parts of the nucleus and cytoplasm, respectively.

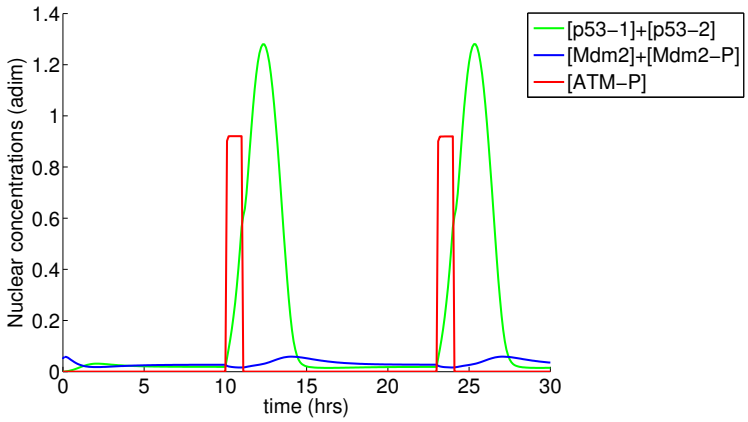

Figure S4: The solution of the RD system (S3)-(S4) where the steady-state solution is perturbed at the 10 and 23 hour time points by the activation of ATM for one hour. After a high amplitude excursion of the p53 concentration from its steady-state, p53 returns to the steady state again.

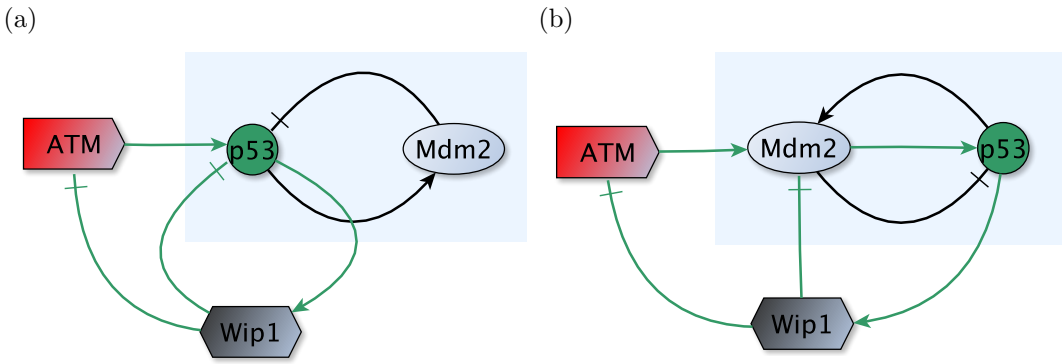

Figure S5: (a) The feedback loops used in the model [17]: the classical $p53 \to Mdm2 \dashv p53$ where p53 induces transcriptionally Mdm2 and Mdm2 degrades p53 and the loop between ATM and Wip1 with the intermediate p53 protein, i.e. $ATM\text{-}P \to p53 \to Wip1 \dashv ATM\text{-}P$. (b) The feedback loops used in the model with the dual function of Mdm2 towards p53: $p53 \to Mdm2 \dashv p53$ and the loop between ATM and Wip1 through the cascade involving p53 and Mdm2, i.e. $ATM\text{-}P \to Mdm2 \to p53 \to Wip1 \dashv ATM\text{-}P$, where Mdm2, after being phosphorylated by ATM, enhances synthesis of p53 which, in turn, activates transcriptionally Wip1 (and also Mdm2) which inactivates ATM. *In the sketch, the "+-shaped" lines denote negative regulation and the classical arrows denote positive regulation (of either activity or expression).*

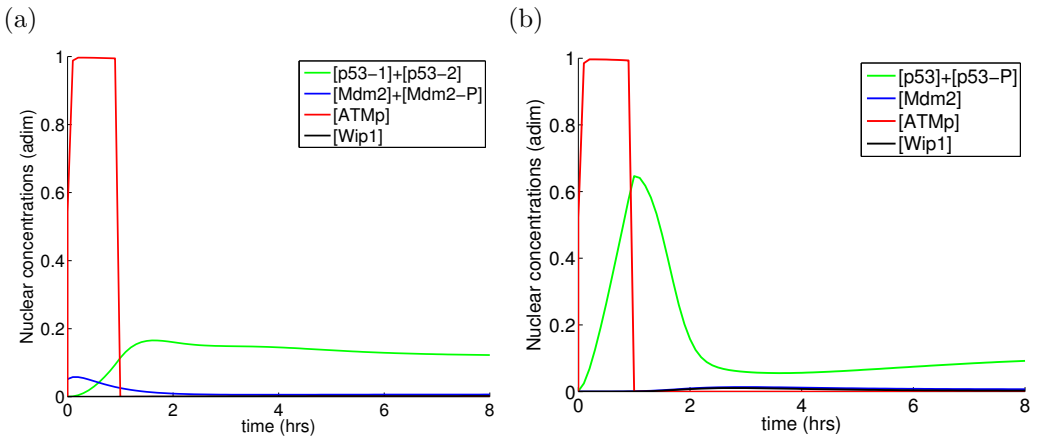

Figure S6: (a) Solution of the RD system (S3)-(S4) modelling p53 dynamics *with* the dual function of Mdm2 towards p53 when $k_a = 0$, i.e., no complexes between p53 mRNA and Mdm2-P are allowed, and ATM-P signalling is inhibited 1 hour after damage. (b) Solution of the RD system in [17] modelling p53 dynamics *without* the dual function of Mdm2 towards p53 and when ATM-P signalling is inhibited 1 hour after damage.